Volume 1 | Number 1 | Jan 2013 | Pages 1–100

Integrative Biology

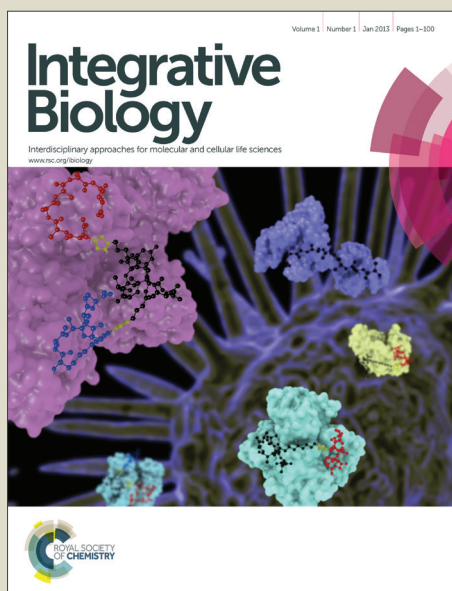Interdisciplinary approaches for molecular and cellular life sciences
www.rsc.org/ibiology

ROYAL SOCIETY OF CHEMISTRY

This is an *Accepted Manuscript*, which has been through the Royal Society of Chemistry peer review process and has been accepted for publication.
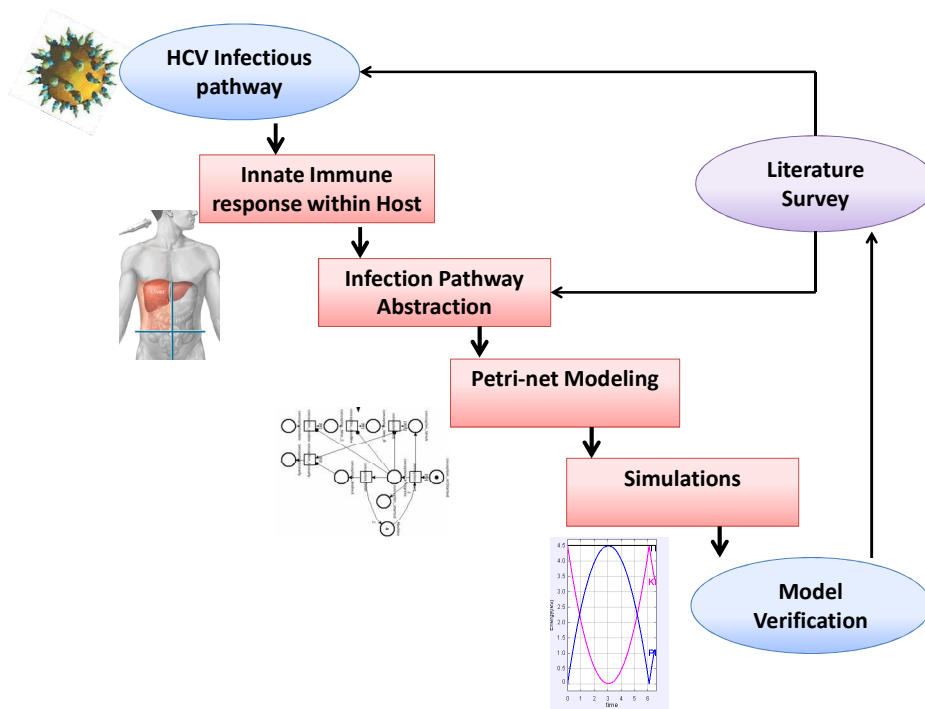
Accepted Manuscripts are published online shortly after acceptance, before technical editing, formatting and proof reading. Using this free service, authors can make their results available to the community, in citable form, before we publish the edited article. We will replace this *Accepted Manuscript* with the edited and formatted *Advance Article* as soon as it is available.

You can find more information about *Accepted Manuscripts* in the **Information for Authors**.

Please note that technical editing may introduce minor changes to the text and/or graphics, which may alter content. The journal's standard **Terms & Conditions** and the **Ethical guidelines** still apply. In no event shall the Royal Society of Chemistry be held responsible for any errors or omissions in this *Accepted Manuscript* or any consequences arising from the use of any information it contains.

Insight, Innovation, Integration

The exact mechanism by which HCV evades the immune responses of the host is not well defined. Current research highlights defects at multiple levels of the immune responses and involvement of various cellular and viral genes. In order to understand immune response failure in clearing HCV, we present a simplified formalization of the highly dynamic system consisting of HCV, its replication cycle and host immune responses at the cellular level using Petri Nets. The current study deals with step wise simulation, model validation and analysis of host immune response estimation against HCV. The study tries to make correlations among viral RNA levels, interferon production and interferon stimulated genes induction. The simulations are in agreement with the published expression studies and western blot experiments. Our proposed methodology provides valuable insights to assess other integrated pathways in biological systems. It is simplified, biologist friendly approach integrating virology, immunology and systems biology. Furthermore, it will greatly help in devising experiments and predicting dynamic behavior of the proteins involved in specific signaling pathways.

Schematic outline describing HCV PN model generation and its verification

Table of Contents

Modeling and analysis of innate immune responses induced by the host cells against Hepatitis C Virus infection

Ayesha Obaid[a], Jamil Ahmad[b], Anam Naz[a], Faryal Mehwish Awan[a], Rehan Zafar Paracha[a], Samar Hayat Khan Tareen[b], Sadia Anjum[a], Abida Raza[c], Jan Baumbach[d] and Amjad Ali[a] *

[a]Atta-ur-Rahman School of Applied Biosciences (ASAB), National University of Sciences and Technology (NUST), Islamabad, 44000 Pakistan
[b]Research Center for Modeling and Simulation (RCMS), National University of Sciences and Technology (NUST), Islamabad, Pakistan
[c]Nuclear Medicine Oncology & Radiotherapy Institute (NORI), Islamabad, Pakistan
[d]Dept. of Mathematics and Computer Science, University of Southern Denmark, Campusvej 55 DK-5230, Odense M, Denmark

* Corresponding author
Atta-ur-Rahman School of Applied Biosciences (ASAB),
National University of Sciences and Technology (NUST),
H-12, Islamabad, 44,000 Pakistan
E-mail: amjad_uni@yahoo.com

Abstract

An in-depth understanding of complex systems such as hepatitis C virus (HCV) infection and host immunomodulatory response is an open challenge for biologists. In order to understand the mechanisms involved in immune evasion by HCV, we present a simplified formalization of the highly dynamic system consisting of HCV, its replication cycle and host immune responses at the cellular level using hybrid petri net (HPN). The approach followed in this study comprises of step wise simulation, model validation and analysis of host immune response. This study was performed with an objective of making correlations among viral RNA levels, interferon (IFN) production and interferon stimulated genes (ISGs) induction. The results correlate with the biological data verifying that the model is very useful in predicting the dynamic behavior of the signaling proteins in response to a stimulus. This study implicates that the HCV infection is dependent upon several key factors of the host immune response. The effect of host proteins on limiting viral infection is effectively overruled by the viral pathogen. This study also analyzes activity levels of RNase L, miR-122, IFN, ISGs and PKR induction and inhibition of TLR3/RIG1 mediated pathways in response to targeted manipulation in the presence of HCV. The results are in complete agreement at the time of writing with the published expression studies and western blot experiments. Our model also provides some biological insights

regarding the role of PKR in the acute infection of HCV. It might help to explain why many patients fail to clear acute HCV infection while others, with low ISGs basal levels, clear HCV spontaneously. The described methodology can easily be reproduced, which suitably supports the study of other viral infections in a formal, automated and expressive manner. The petri net-based modeling approach applied here may provide valuable insights for study design and analyses to evaluate other disease associated integrated pathways in biological systems.

1. Introduction

Hepatitis C virus (HCV) is the causative agent of hepatitis C infection, which is an infectious liver disease of human, conclusively studied in 1989 for the first time [1]. HCV is an enveloped positive-strand RNA virus which belongs to the family *Flaviviridae* [2]. According to the recent data, seven major HCV genotypes and more than 67 subtypes have been identified [3]. Population based estimates indicate that ~200 million people are chronically infected globally with HCV and are at a risk of developing chronic liver disease including cirrhosis and hepatocellular carcinoma[4]. Over 0.3-0.5 million deaths occur each year due to HCV and related complications [5]. Among HCV infected patients, 10–30% can be cured spontaneously [6] while 40-70% of chronic cases achieve sustained virological response (SVR) to pegylated interferon-alpha and ribavirin (Peg-IFN-α/RBV) treatment [7]. The degree of treatment response is majorly dependent upon the infective genotype [8], thus Peg-IFN-α/RBV therapy usually provides limited efficacy and is poorly tolerated in genotype-1 because of its non-specific nature [9]. To overcome this limitation, triple therapy has been introduced to treat resistant genotypes and advanced stages of HCV infection [10]. It includes the use of direct-acting antiviral agents (DAAs) with or without Peg-IFN-α/RBV. Approved DAAs recently include sofosbuvir, boceprevir and telaprevir[10]. The use of DAAs has made promising progress in the treatment of HCV but the issue of drug resistance and profound side-effects in a significant proportion of the patients often results in a premature cessation of the treatment [10, 11]. So far, there has been little success in developing an effective prophylactic vaccine against HCV because of its high mutation rate and the presence of quasispecies [12, 13].

Chronic viral infection indicates that HCV has evolved efficient defensive mechanisms to escape the immune system and interfere with the host immune mechanisms. HCV has developed various strategies including genomic variability, adaptability and its multifunctional proteome [14]

to evade both innate and adaptive immune responses. This situation emphasizes the need for well-defined antiviral and immune modulatory therapeutics to achieve HCV-specific immunity [15]. The complexity and the wide range of host-pathogen interactions and interlinked signaling pathways at cellular level make it very difficult and expensive to study them on a broad-scale. The understanding of these complex interactions is limited due to the difficulties in cell culture propagation[16]. The vast amount of data generated over the last decade, regarding HCV cell signaling and molecular interactions needs to be analyzed in greater detail in order to formulate a comprehensive delineation of this devastating virus.

Cell signaling is part of a complex system of communication that governs basic cellular activities and coordinates cell actions. Information flow within a cell is carried out by these cell signaling networks through various processes of activation and de-activation of proteins present in the signaling cascade. Either it is through small messenger molecules or phosphorylations and de-phosphorylation of proteins by kinase enzymes. It is important to note that such signaling networks have signal flow but no substance flow. These signaling networks are complex systems in their organization and deciphering the exact flow of signals or events through such networks is a complicated task. Hepatitis C infection is similarly a complex disease in which several intertwining signaling cascades play crucial role in establishing a complex network resulting in diseased state. These cellular signaling and molecular interaction networks can be interpreted and analyzed using a number of systems biology techniques including small-scale differential equation approaches or graphs [17].

Ordinary differential equations (ODEs) are usually limited to small-scale networks given the difficulty in obtaining the numerical values of kinetic parameters and standardization of the parameters and models [18]. On the other hand, systems biology techniques based on graphs focus on the structure of the constructed cellular network or given signaling pathway, by computing the prominence of different components and processes. These approaches provide a static view of the network along with finding alternative pathways, junctions, crosstalk, and hubs [17]. However, such techniques also limit themselves by ignoring the behaviors that the system can exhibit. Dynamic analyses cover these limitations by adding the behavioral dimensions to the constructed network [19]. Two prominent techniques which are employed for this purpose arelogical modeling [19] and Petri Nets (PN) [20]. In terms of the type of analyses, logical modeling caters to discrete and hybrid approximations of the systems, whereas PN can provide discrete,

hybrid, or continuous approximations[20]. Although both are applicable for most biological networks, PN have a slight edge over the logical modeling approach because of their ability to model a large number of entities and components within a single system, whereas logical modeling methodologies tend to suffer from state space explosion - an increase in complexity of the system with increasing number of entities [21]. This state space explosion effectively limits the number of components of the system to less than 7 [21]. Since our modeled system (HCV infection pathway) comprises of 23 entities, PN serve as the most efficient and effective method of modeling and analysis. PN modeling provides a generic description principle which can be applicable to any level of abstraction[22].

Our study proposes a PN model of the HCV infection pathway and resultant host innate immune response. We formulated an approach to reduce the noisy biological data and make it convenient to study this disease from a systems level prospective. To the best of our knowledge, the systems level study and the PN model of innate immune response against HCV is being reported for the first time. It is based on well documented experimental evidences till date [2, 3, 8, 9, 14, 15, 23-31]. Our study tries to encompass the important host immune signaling pathways involved in the innate immune response to HCV infection and thus explains the factors responsible for the evasion of HCV from host immune responses. The studied pathways include ribonuclease L (RNase L), microRNA-122 (miR-122), toll like receptor 3 (TLR3), retinoic acid-inducible gene 1 (RIG1) and protein kinase R (PKR) pathways. Our proposed model and the results of targeted experiments reflect the behavior of the proteins correctly when subjected to specific perturbations.

2. Material and methods

2.1. Petri Nets

A Petri Net can be defined as a directed bipartite graph having two distinct sets of nodes (places and transitions). The places are represented by circles, whereas the transitions are represented by boxes or bars. Usually, places are used to describe resources (for example entities like proteins, mRNAs etc.) and their states (levels, number, concentration etc.). In contrast, transitions represent interactions or processes occurring in the system. Being a bipartite graph, the arcs or edges, represented as directed arrows, connect only distinct nodes, that is only places to transitions and vice versa. The weight of an arc (by default, 1) represents the arc multiplicity.

'Inhibitory edges' are used to suppress the flow of tokens and thus stops the firing of a transition. They are represented by an arc with a hollow dot as its head (———o) [32-34]. Places incident (predecessors) to transitions are said to be input places whereas places successor to transitions are output places for that particular event. The number of places can neither be infinite nor zero in a PN [32].

Tokens are variable elements of a PN inside places. They are indicated as dots or numbers within a place and represent states of entities [35]. In a biological system, tokens may refer to concentration levels or a discrete number of a species, e.g., proteins, RNA transcripts, ions, organic and inorganic molecules [32]. The state of the system is therefore represented by the available tokens in the places at a particular instance of time and is also called the 'marking' of the system at that instance. The initial marking of the PN allocates a number of tokens to each place which may or may not enable respective transitions, depending on whether the tokens in the places satisfy the weights of the arcs connecting the said places to the respective transitions.

As mentioned earlier, a transition represents an event or a relation between two or more places. It changes the state of input and output places connected to it, depending upon the state of the resource. A transition without an input place is said to be a 'source transition' and the one without output place is called a 'sink transition' [36]. Firing of a transition withdraws a number of tokens from the input place and deposits it to the output places according to respective arc multiplicities [20]. Token flow within the model actually represents the dynamic evolution of a PN (and by extension, of the underlying system).

Formally, A Petri net is a 3-tuple (P, T, W), where:

- *P* is a finite set of places;
- *T* is a finite set of transitions;
- *W* is a set of arcs, connecting a place to a transition or vice versa. No arc may connect two places or two transitions.

In this study, SNOOPY version 2.0 [33] for windows was used for PN model generation and simulations. It is a unified PN tool which has various modeling options available. We employed a Hybrid Petri Net (HPN) in this study as it supports real numbers, and continuous modeling while allowing us to clearly express the relationship between continuous values and discrete

values, keeping the good characteristics of the discrete PN sound [35]. After the model was completed, arc weights and mass function rates were adjusted according to the requirement of the respective pathway (based on experimental evidences). The final PN model was then subjected to model checking and analysis tools available in Snoopy v 2.0 [33].

2.3. Non-Parametric Strategy for PN modeling

There are various reported studies employing PN approaches for modeling cellular signaling cascades and gene regulatory networks [37]. Each group[22, 32, 34] has tried to extend this formalism to encompass the complexity of the cellular environment. Our study is based on the non-parametric strategy devised by Ruths *et al.*, [38] for studying the dynamics of cell specific signaling pathways employing PN approaches. The PN model is based on the assumption that the signaling network connectivity is the most significant determinant of signal propagation[37]. Therefore, changes in the activity levels of the proteins within a particular signaling pathway correlated with their abstract quantities represented in the PN model by token number [38].

2.4. Construction of the Petri Net

In a signaling pathway, rules of a chemical reaction cannot always be applied. A signaling cascade is activated by the entry of a foreign particle in the cell, which in turn activates the enzymes already present in the system by phosphorylation, de-phosphorylation, physical protein-protein interaction or any other post-translational modification. In order to model such a pathway, a modeling strategy was devised for each process which best suited the topology of the HCV infection model.

In the designed PN model (**Figure 2 and 4**), places represent the proteins and genes (e.g. cellular enzymes, HCV structural and non-structural proteins, transcription factors, and immune modulatory proteins etc.) involved in innate immune signaling pathway whereas the transitions describe the processes, interactions or reactions occurring in between the places (e.g. chemical reactions, complex formation, gene silencing, gene enhancing, de-/activation, de-/phosphorylation, transcription, transport processes etc.). Two types of places are used in our model, continuous and discrete places. The markings of continuous places are real numbers and the firing of transitions is a continuous process while discrete places have a finite number of tokens. All the arcs have weight equal to 1 except for those mentioned otherwise. Inhibitory arcs are used here to show inhibitory effects of HCV proteins on certain cellular processes or proteins. In our model the source transitions can be interpreted as the synthesis/availability of the

proteins involved in the signaling pathways, whereas sink transitions can serve as an abstract description of dissociation or decay of the compounds leaving the system.

In our study, the combinations of input and output arcs are determined exclusively by the type of molecular interaction and the cellular process involved. Therefore, various combinations of input and output arcs are used to model the different biochemical processes that mediate protein-protein interactions in a signaling network. These processes may include post-translational modifications, enzymatic activation, translocation, complex formation etc.

In our study, the model was designed to find the relative activity change (up-regulation/down-regulation) and not the exact measurement of the protein concentration/parameters within HCV signaling pathway. In biological systems, tokens refer to a relative concentration level or a discrete number of a species, e.g., proteins, RNA transcripts, ions, organic and inorganic molecules. In order to simulate the system, we needed to indicate the availability of the proteins and other entities in the system. Accordingly, the initial values of the tokens were assigned to the entities (present in the HCV signaling pathway) corresponding to a basal state (relative concentration in the cell). Furthermore, the model was simulated for various number of initial tokens (10, 50, 100 etc.) for the entities (receptors, enzymes, co-factors) and simulation graphs were compared, which led to the conclusion that varying initial token value has little to negligible effects on the relative behavior of proteins (**Supplementary File 6A, 6B, 6C, 6D**). The steps involved in the PN model generation include; literature survey to extract the most important determinants of innate immune response against HCV infection; iterative abstraction of the extracted pathway; PN model generation; analysis and verification of the model.

2.5. Abstraction of the HCV infection pathway (KEGG)

The complexity of the biological pathways renders it very difficult to study the kinetic parameters of each reaction between entities due to the limitation of analytical procedures [16]. The phenomenon of state space explosion is very common in the analysis of complex biological pathways [39], which are interlinked at diverse points, each affecting the other in a different way in various situations. Thus, in order to reduce the pathway as presented in KEGG database (pathway ID hsa05160, **Supplementary File 1**) [40], we analyzed and isolated those key points which play the most important role in the induction of interferon-β (IFN-β) as well as interferon stimulated genes (ISGs) (**Figure 1**). Literature data and in-depth analysis revealed RNase L, RIG1, and TLR3 pathways being most essential in stimulating an antiviral response. After

limiting the PN to these pathways, we applied the iterative abstraction strategy as discussed by *Paracha* et al.,[41]. Briefly, one such example stated that if an entity A activates another entity B, which in turn activates C which is involved in interaction with another pathway, subsequently we can omit B and represent this relation as A activates C. In the process of reduction, the behavior of the removed entity B was preserved completely in the activation of C via A.
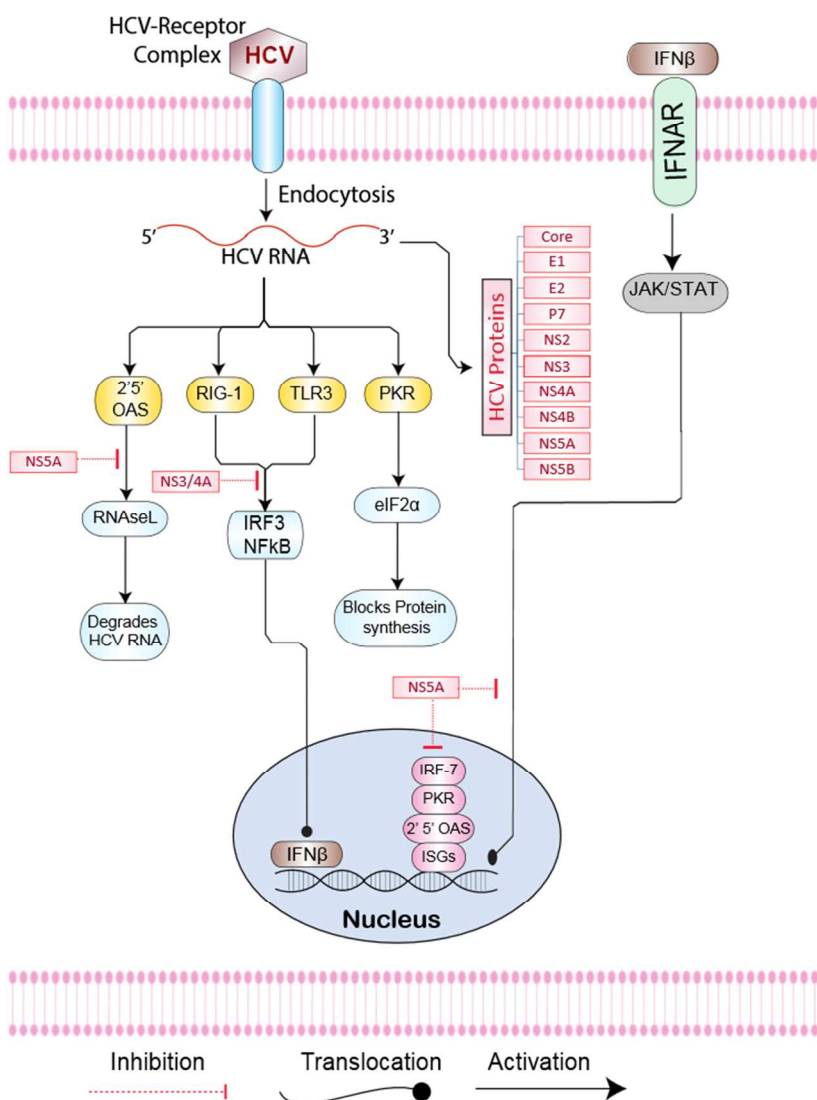

Figure 1: Summarized innate immune signaling cascade during HCV-human hepatocytes infection. This signaling cascade is adapted from KEGG database (pathway ID hsa05160, Supplementary File 1) [40] and supported by experimental evidences. The innate immune response is triggered by the attachment of envelope protein (E2) of viral particle with HCV receptor complex on the hepatocytes surface [42]. After endocytosis, viral genome RNA (+) is released and is translated into 10 HCV proteins [42]. HCV RNA (+,- hybrid genome) is recognized by innate immunity

activating TLR3, RIG-1, PKR and RNase L pathways [8]. TLR3 and RIG1 pathways transduce the signal to the nucleus via upregulation of NF-κB and interferon regulatory factor 3 (IRF3) factors [12]. IFN-β produced as a result of innate immune response is transported outside of the cell creating an antiviral state in the nearby cells. IFN-β induces ISGs via JAK/STAT pathway [43]. ISGs are responsible for limiting viral replication and propagation, RNase L is responsible for degrading viral RNA while PKR induces eukaryotic translation initiation factor 2α (eIF2α) which limits protein translation in the cell [29]. PKR has been recently implicated in supporting viral propagation positively by limiting the translation of ISGs [31]. HCV proteins evade immune response by intervention of TLR3, RIG-1, RNase L and PKR pathways [29]. NS3/4A protease blocks RIG1 and TLR3 pathway by degrading IPS1 and TRIF adaptor proteins thus limiting IFN-β production [13]. NS5A inhibits RNase L and JAK/STAT pathways leading to downregulation of ISGs, enhancing viral propagation [44].

2.6. Modeling approach for HCV infection pathway

Lifecycle of HCV begins with its entry into the hepatocytes. HCV entry is mediated by a complex arrangement of HCV receptors on the cell surface. These receptors include low-density lipoprotein (LDL) receptors, CD81 (Cluster of Differentiation 81) tetraspanin [45], the scavenger receptor class B type 1 (SR-B1) [46] and the tight junction proteins, claudin-1 and occludin [47, 48]. They are represented by a single discrete place depicting a receptor complex. Following internalization via clathrin-dependent endocytosis, the next steps include uncoating and release of the viral genome i.e. RNA (+) [42]. Once the HCV genomic RNA has entered the cytoplasm, it is translated into a single polyprotein. HCV RNA genome contains a single open reading frame of 9.6Kb, flanked by untranslated regions (UTRs), encoding for a single large polyprotein of ~3000aa. The polyprotein is produced directly using an internal ribosome entry site (IRES) dependent translation mechanism in the host cell cytoplasm present within the 5' end of the HCV genome. The polyprotein is further processed by cellular and viral proteases to produce structural as well as non-structural proteins [49]. Core protein forms the nucleocaspsid; E1 and E2 form the envelope proteins; P7 acts as a viroporin; NS2 is a transmembrane protein; NS3 codes for metalloprotease, helicase and serine protease; NS4A acts as a co-factor for NS3 protease; NS4B helps in the replication complex formation; NS5A is a zinc-containing phosphoprotein involved in the regulation of HCV RNA replication; NS5B is RNA-dependent RNA polymerase [49]. After virion maturation, it is released outside the cell via exocytosis. Several host cell factors (replication , translational machinery, receptors etc.) are required and used throughout the virus translation, replication, production and subsequent release [50].

Following HCV infection in the hepatocytes, host immune system is stimulated in response to the presence of viral RNA (dsRNA). Viral degradation by host factors is a well-

established innate immune mechanism to halt the viral translation and replication. RNase L (2-5A-dependent RNase) is activated in response to the presence of foreign RNA. It not only degrades HCV RNA but also helps in stimulating IFN response [30]. Upon infection several pattern recognition receptors (PRRs) are stimulated such as TLR3 and RIG-I-like receptors (RLRs) which eventually lead to the induction of type I IFN production and ISGs through the activation of interferon regulatory factors IRF7 and IRF3. Secreted IFNs induce an antiviral state that extends to the non-infected neighboring cells. IFN induction leads to activation of the JAK (Janus kinase)/STAT (signal transducer and activator of transcription) signaling pathways [26, 43].

Despite such robust antiviral response mechanisms of the host cell, HCV proteome activates and deactivates several host pathways to enhance viral entry, replication and thus escape host immune response. NS5A protein of HCV blocks the RNase L mediated RNA degradation by interacting with 2′,5′-oligoadenylate synthetase (2-5OAS) thus inhibiting its antiviral activity [44]. Liver-specific miR-122 binds at two sites within the 5′-UTR of HCV RNA which positively regulates the viral life cycle, in part by stimulating HCV translation [51]. The NS3/4A protease, which cleaves the TIR-domain-containing adapter-inducing interferon-β (TRIF) and IPS1 (IFN-beta promoter stimulator 1) proteins, inhibits TLR3 and RIG1 mediated IFN production respectively [52]. Taken together, HCV has developed sophisticated ways to anticipate, weaken and antagonize immune responses (see **Figure 1**). Understanding the mechanisms by which HCV circumvent the innate and adaptive immune systems not only provides important clues about how the virus adapts to the host environment but also opens new perspectives for preventive and therapeutic strategies based on the improvement of innate and acquired immune responses. The Hybrid Petri Net (HPN) class was used to model this innate immune response mechanism against HCV in a step-wise manner employing the abstraction strategy discussed earlier (**see section 2.1.**).

2.7. Model verification through simulations

Every constructed model has a set of all possible behaviours which the model can exhibit. This set constitutes the state space of the model [53]. Discrete models have a finite state space and can be studied to find different behaviours. In contrast, continuous models have a very dense, and often infinite state space, which is usually approximated to discrete or hybrid equivalents [54]. Model checking (automated model verification methods) utilizes this state space to check whether certain properties and behaviors are present in it [55]. One of the advantages of PN is that

it can simulate the Place/transition net with the flow of tokens in the system. It can give approximate prediction of the dynamical properties of the model with time.

Simulative model checking approaches handle the state space through approximating results by analyzing only a subset of the state space. It is also possible to perform multiple simulation runs and observe the mean result of all runs. Thus, an averaged time course will be computed, with higher number of simulation runs contributing to the precision of the averaged time course. All single simulation runs will fluctuate around the averaged time course. Thus, even a model with an infeasible or infinite state space can be subjected to model checking. Our approach utilizes such simulation runs to validate the pathway model.

In order to verify our model, we focused on some of the essential properties (replication, translation, interferon production) of the HCV infection pathway (**Table 1**) which have been experimentally validated. Comparison of our simulation results with already proven protein expression data for HCV signaling pathway, corroborated the earlier findings involving TLR3 and RIG1 pathway inhibition by HCV proteins. In essence, the tokenized activity-levels computed by our method should be taken as abstract quantities whose changes over time correlate to changes that occur in the concentrations of active proteins present in the cell. Thus, getting similar results as of experimental values from our designed model actually validates the soundness of the model. Hence this model can be used and extended for the identification of various other biological insights related to HCV signaling pathways (**see section 3.6**.). Following a similar methodology, biologists can estimate and explore the interactions among group of entities in a cell, supported by their respective properties and biological functions, as well as system-level perspective for various diseases prior to spending time and resources in wet lab experiments.

3. Results and Discussion

The significance of a quantitative model cannot be denied but the limitations of available kinetic data for each entity in the complex signaling pathways renders it very difficult to formulate the extensive model. Here an HPN model of HCV infection is presented encompassing TLR3, RIG1, and RNase L mediated signaling pathways. In order to develop the HPN model, it is assumed that HCV particles are continuously present in the blood and HCV receptor complex is readily available for internalization of HCV particle. As soon as the HCV particle is internalized, it starts

translation of its proteins by utilizing host cellular machinery. Simultaneously, when foreign dsRNA is detected by the PRRs, innate immune response is activated. We also assume that there are abundant nucleotides and amino acids in the cell so that cellular resources do not limit HCV RNA replication and translation. Thus, if any cellular components are needed to form the replication machinery or are required for the production of viral proteins, they are readily available. The tokens in the places of this model only represent the presence of an entity and do not attribute to the actual concentration of an entity. Mass action kinetics with rate = 1 are used for all reactions and processes, except for HCV replication where the rate is 0.5 to compensate for other processes utilizing HCV RNA such as translation and virion production. Time units represent specific time blocks during which each transition is fired once. These blocks are either optimized through laboratory experiments or through literature. Time units may depict minutes, hours or days depending upon the particular type of experiment.

The complete HPN model of HCV infection representing the summarized pathway (**Figure 1)** is illustrated in **Figure 2 and 3**. **Figure 2** represents the initial phase of HCV infection pathway in the host hepatocytes, resulting in the activation of host innate immune response to limit viral replication. It consists of total 23 places 18 transitions, and 52 edges.
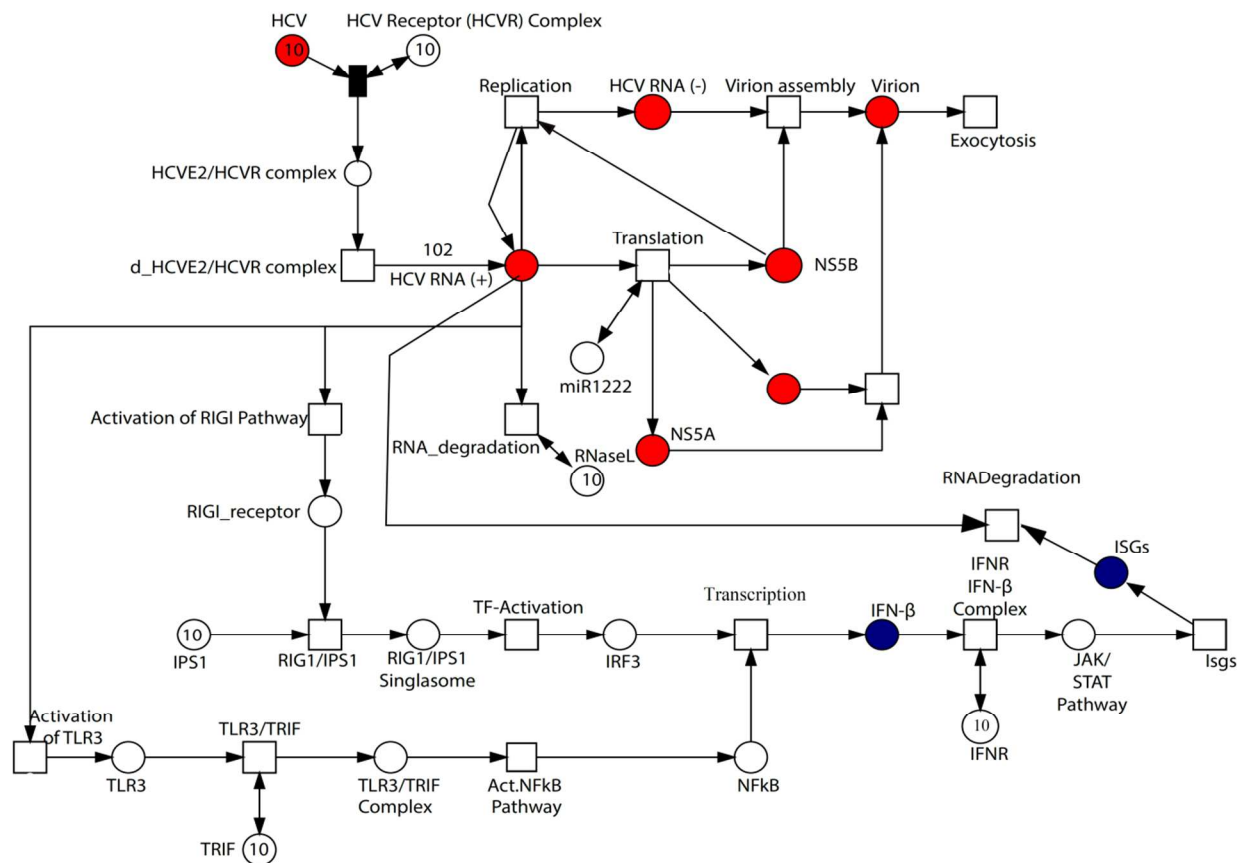
Figure 2: **Illustration of the HPN model representing HCV infection and host immune response**. A standard place is illustrated as a circle ◯ representing HCV proteins, cellular enzymes, and receptor complexes. A continuous transition is depicted as ☐ representing all cellular processes including endocytosis, exocytosis, transcription, translation and activation. A directed arc ⟶ connects a place with a transition and vice versa. Weights of the arcs are equal to 1 unless mentioned otherwise. All native proteins of the cell and HCV particle have been given arbitrary token number of 10. Red places represent important HCV proteins (HCV, HCV RNA, NS5B, NS5A, NS3/4A, virion) selected for this study. Blue places represent important end products (IFN-β, ISGs) of host innate immune response selected for this study in particular. The inhibitory effects of HCV protein on host immune system are shown in **Figure 3**.

The complete pathway (**Figure 2**) is simulated to evaluate the system as a whole. The simulation shown in **Figure 4** represents the entities (proteins, RNA, receptor complexes, genes) involved in the innate immune response against HCV infection (**Figure 2**) and their dynamic behavior with time. Each entity can be exclusively studied through simulations in relation to the viral infection and host response. It gives a complete picture of the system under study. It is observed that as soon as HCV RNA (+) is internalized, it starts translation of its proteins. There is an initial increase in viral RNA and proteins until it is recognized by the host machinery which

activates antiviral responses. e.g. RNaseL is activated and it degrades HCV RNA(+) which results in decline of its concentration. Virion production is relatively low whereas IFN-β and ISGs induction is relatively high. Enzymes (cellular factors) remain constant while they trigger the downstream processes by activation or deactivation of signaling proteins. Several key processes such as HCV RNA replication, translation, innate immune responses and their corelation is studied in detail in the following sections (**section 3.1-3.5**).
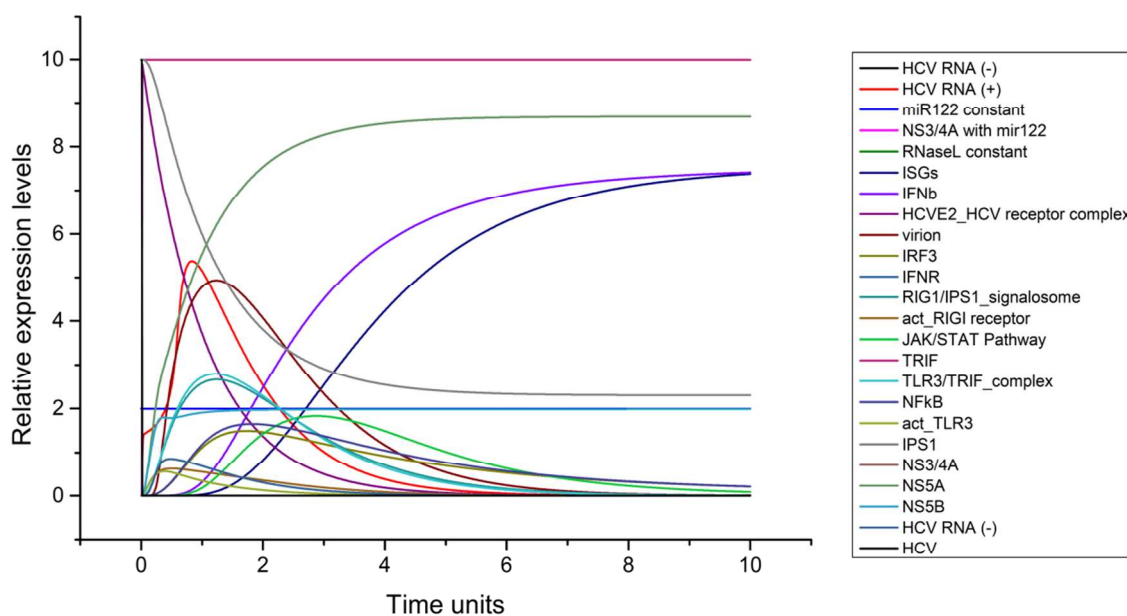

Figure 4: **Collective simulation of 22 entities in HCV innate immune pathway.** X-axis shows time units and Y-axis shows relative expression levels of proteins and RNA in HCV infected hepatocytes. The relative activity level change of each entity is observed in relation to HCV infection and host innate immune response.

In the later phases of HCV infection (chronic), HCV establishes itself in the host and leads to chronic infection by limiting host immune responses [29]. Several HCV proteins are known to inhibit key host immune pathways and assist in evasion of the viral infection from these immune responses [6]. **Figure 3** illustrates the PN model illustrating the phase of HCV infection where the HCV proteins hijack the immune response and inhibit the pathways by either direct interaction or proteosomal degradation. It consists of 53 places, 18 transitions and 56

edges. Red places represent the important proteins of HCV, while red arcs represent inhibitory action. Blue places represent the important end products of host immune response selected for this study (**Table 1**).
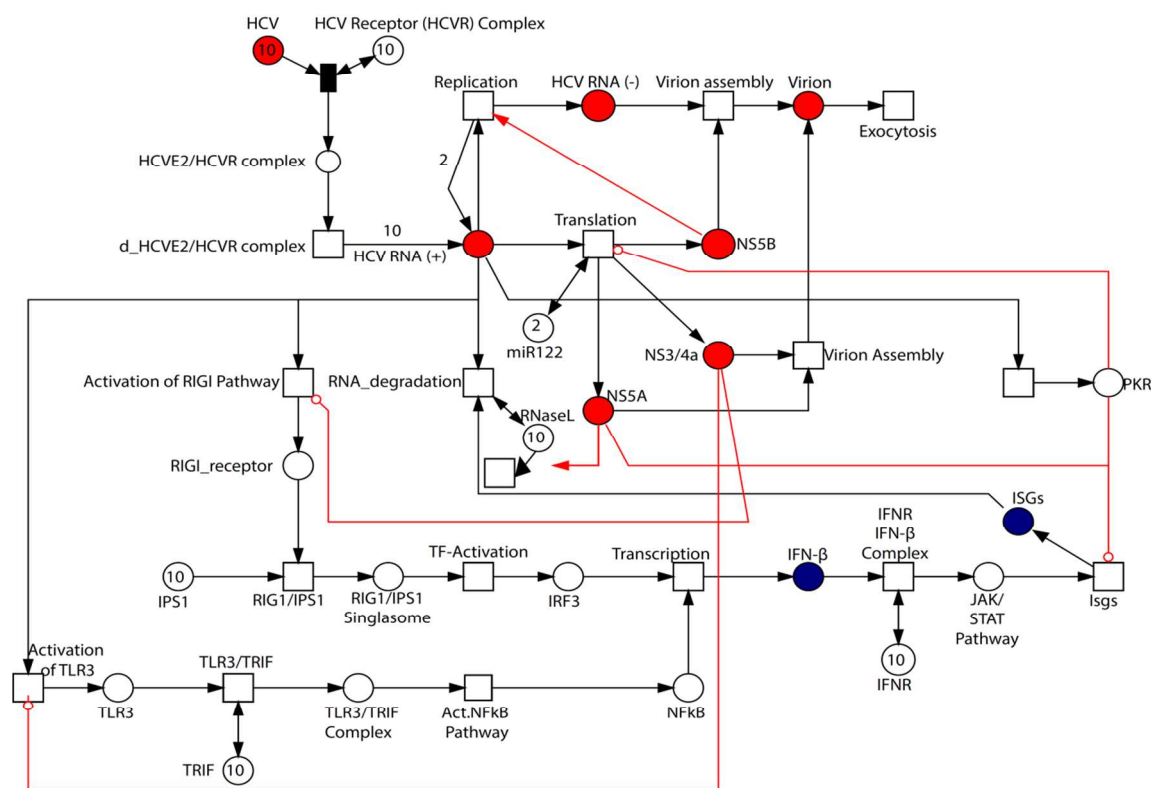

Figure 3: Illustration of the HPN model representing evasion of HCV from host immune response. A standard place is illustrated as a circle ◯ representing HCV proteins, cellular enzymes, and receptor complexes.. A continuous transition is depicted as ☐ representing all cellular processes including endocytosis, exocytosis, transcription, translation and activation. A ⟶ directed arc connects a place with a transition and vice versa. An inhibitory arc ⟶◦ represents the inhibitory effect of HCV proteins on TLR3, RIG1, RNase L, PKR and ISGs induction. ⟶ is a directed arc but represents the inhibitory effect of HCV proteins by activation mechanisms. Red places represent important HCV proteins selected for this study. Blue places represent important end products of host immune responses selected for this study in particular.

The simulation of HPN model (**Figure 3)** is represented in **Figure 5.** It shows the behavior of host and viral entities after virus takes over the host machinery for its survival and propagation. Critical changes in the behavior of several entities are observed when simulation of

the HPN model (**Figure 3**) is analyzed. As the host pathways are inhibited, IFN-β and ISGs are reduced in the cell whereas HCV proteins translation and virion production is accelerated. After critical analysis of the complete simulation few important processes were selected for detailed analysis (**summarized in Table 1**). The comparison of IFN-β, ISGs, HCV proteins, HCV RNA under two different situations is critically analyzed in detail (sections 3.1-3.5).
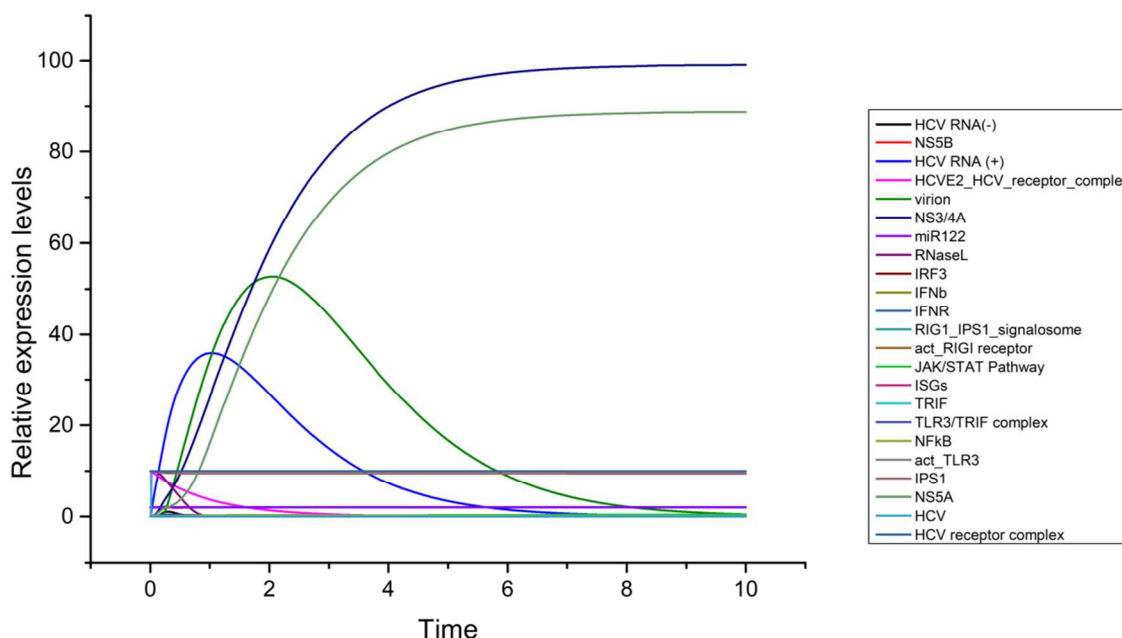

Figure 5: Collective simulation of 22 entities after hijacking of immune responses by HCV proteins. X-axis shows the time units while Y-axis represents relative expression levels. The relative activity level change is observed with time in relation to the inhibition of innate immune response pathways (RNaseL, TLR3, RIG-1). The graph shows that host responses are downregulated (IFN-β, ISGs) while viral proteins and virion production is relatively upregulated (HCV RNA , NS3/4A, virion, etc).

In the next step the differences in between HPN models (**Figure 2, 3**) were analyzed by comparing simulation graphs of several key entities individually, in order to elaborate the effect of HCV proteins on innate immune pathways. Each entity in the pathway was compared in both the PNs representing two types of situations. One, in which host innate response is in full burst while in the other, HCV takes over the host machinery. **Figure 6** represents the comparison of relative change in activity levels of entities in both PNs (**Figure 2, 3**).
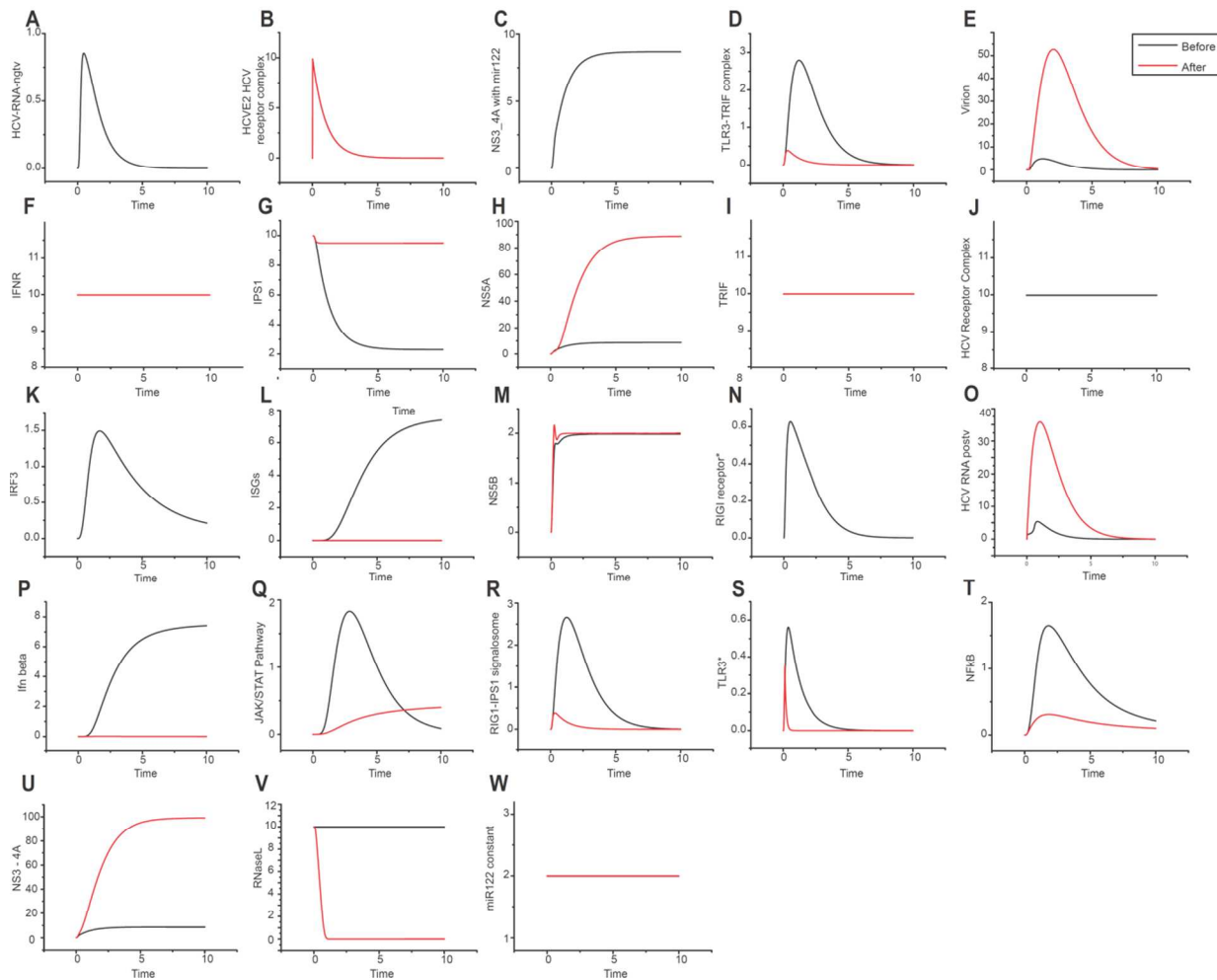
Figure 6: Comparison of relative change in the activity levels of entities in HCV infection and innate immune response. X-axis shows time units while Y-axis shows the relative activity level change in the entities compared in two PNs **(Figure 2, Figure 3).** Black line represents the relative activity level before any HCV inhibitory effect is observed while red line shows the relative activity level after HCV proteins affect the innate immune response pathways. The effects observed here are due to the introduction of inhibitory arcs in the pathway; 6A represents the relative level of HCV RNA (-) before and after inhibition by HCV proteins; 6B represents HCV E2 attachemnt to receptor complex and entry into the cell; 6C represents NS3/4A level with miRNA 122; 6D represents TLR3/TRIF complex; 6E represents virion production; 6F represents interferon receptor (IFNR); 6G represents IPS-1; 6H represents NS5A level; 6I represents TRIF; 6J represents HCV receptor complex on cell surface; 6K represents IRF3 levels; 6L represents ISGs levels; 6M represents NS5B levels; 6N represents RIG-1 receptor complex; 6O represents HCV RNA (+), 6P represents the level of IFN-β; 6Q represents JAK/STAT pathway; 6R RIG-1/IPS-1 signalosome; 6S represents TLR3 pathway; 6T represents the level of NFκB; 6U represents NS3/4A levels; 6V represents RNaseL level; 6W represents the miR122 level. Horizontal straight lines represent constant level of enzymes or ezyme complexes.

In **Figure 6,** black line represents the relative expression levels of entities present in the pathway before any inhibitory action of HCV proteins occurs[56] while red line represents the relative levels after HCV inhibits RNaseL, RIG-1 and TLR3 pathways[29]. No significant change is observed in **Figure 6A, 6B, 6C, 6F, 6I, 6J, 6K, 6N** and **6W**. It is due to the conserved nature of these proteins, which are present in the cell and perform the "switch on" and "off" functions. After the inhibition of immune responses, the following observations are revealed by analyzing **Figure 6**. TLR3-TRIF is downregulated as a result of proteosomal degradation by NS3/4A protease of HCV[6] in **Figure 6D**. In **Figure 6E**, virion production is upregulated (red) after RIG-1 and TLR3 pathways are inhibited[56]. IPS-1 is an adaptor protein, and is blocked by NS3/4A[6], thus it doesnot take part in the activation of RIG-1 pathway and remains constant (red) in **Figure 6G**. In **Figure 6H,** NS5A production is relatively increased (red line) as compared to NS5A (black). In **Figure 6L,** ISGs are downregulated (red line) and IFN-β is decreased (red line, **Figure 6P)** after HCV inhibits their signalling pathways[26]. In **Figure 6O,** HCV RNA(+) is relatively increased (redline) as compared to the black line indicating robust viral replication after innate immune responses are impeded. JAK/STAT pathway (**Figure 6Q**, red line) and TLR3 pathway (**Figure 6S**, red line) are blocked by HCV proteins and show a relative decrease in later phases of HCV infection. Similarly NFκB is reduced (red line in **Figure 6T**) and NS3/4A is increased (**Figure 6U,** red line) in later phases of infection. **In figure 6V**, RNase L is degraded (red line) when HCV NS5A protein inhibits its pathway[44].

The changes in the behaviors of key entities observed in **Figure 6** led to the selection of few important case studies for detailed examination and verification of the model. The differences in both scenarios (**Figure 2 and 3**) were narrowed down to few of the most important proteins involved in HCV infection and host immune response pathways. Importantly, we have kept our focus on the differences in the relative levels of various viral and host proteins when perturbations were introduced at specific levels in the model. This study is non-parametric based analysis, thus estimation of kinetic parameters is not considered. The model is developed in a step wise manner to analyze the effect of each sub-pathway separately.

3.1. HCV RNA replication

Once the HCV positive stranded RNA {RNA(+)} enters the cells, it forms a complex with ribosome and a single polyprotein is produced which is subjected to viral and host proteosomal cleavage producing viral structural and non-structural proteins [42]. This RNA (+) is also used as a template to produce negative stranded RNA {RNA (-)} by the action of viral specific protein NS5B (RNA dependent RNA polymerase). The HCV RNA (-) in turn acts as a template for HCV RNA replication. The HPN representation of HCV replication is shown in **Figure 2** while its simulation is shown in **Figure 7.** Simulations were analyzed for different values of Mass action kinetics and the parameter was adjusted accordingly. A mass action kinetics rate of 0.5 is used for replication in order to compensate for other processes utilizing HCV RNA. It was optimized after a number of hit and trial attempts. It needed to be adjusted because HCV RNA (+) is used for a number of processes during the infection, such as viral RNA replication, viral RNA translation into HCV proteins and virion assembly[50].

As it is observed in **Figure 7,** the HCV RNA (+) (red) increases exponentially at the start of the process and the HCV RNA (-) (blue) also shows a smaller peak at the same time but the rate of HCV RNA (-) replication is slower than HCV RNA (+). The explosive replication at the start of the process is due to the positive feedback in the model. miR-122, a liver-specific microRNA, which among its many roles, supports viral RNA replication by stabilizing the HCV RNA (+) [28]. As the HCV RNA (-) is not known to bind miR-122 or any other microRNA thus it has a slower replication rate as compared to HCV RNA (+) [28]. However, as evident in **Figure 7**, the degradation rate of HCV RNA (+) is much faster than HCV RNA (-). HCV RNA(-) is known to only function as a replication intermediate thus, it may never be actively released from the membrane bound replication compartment and therefore be protected from degradation in the cytoplasm [28]. Additionally, the 5′ stem structure present at the end of the HCV RNA (-) may serve to increase its stability [28]. The presence of viral RNA (+) activates RNAses in the cytoplasm which degrades the HCV RNA (+) but the HCV RNA (-) is protected. As a result contributing to the slower degradation rate compared to HCV RNA (+).

It is also been observed in previous studies that the ratio of HCV RNA (+) to HCV RNA (-) in the cytoplasm of hepatocytic cell is approximately 10:1[16, 57, 58]. Other mathematical models [16, 24] for HCV sub-genomic replication have also incorporated this phenomenon to construct kinetic

models of HCV. In the **Figure 7**, the ratio of HCV RNA (+) to HCV RNA (-) is depicted as approaching 10:1 which is in accordance with the published findings in cell culture experiments [58].
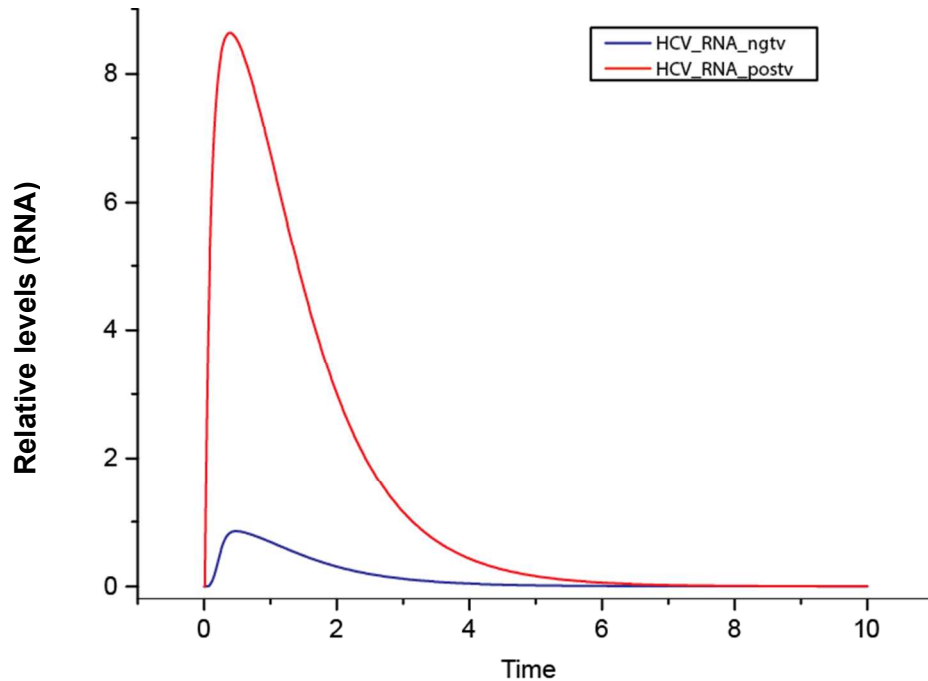

Figure 7: **Simulation of HCV RNA replication {positive strand RNA (+) and negative strand RNA (-)}**. X-axis shows the simulation time units while Y-axis shows the relative expression levels. The red line represents the relative level of HCV RNA (+) while the blue line shows the relative level HCV RNA (-). As indicated by the red line, HCV RNA (+) shows an exponential increase at the start of the process while the HCV RNA (-) (blue) also shows a peak at the same time but the rate of HCV RNA (-) replication is slower than HCV RNA (+). The explosive replication at the start of the process is due to the positive feedback by host microRNA miR-122 [28]. HCV RNA (-) is not known to bind miR-122 or any other microRNA thus it has a slower replication rate as compared to HCV RNA (+). However, the degradation rate of HCV RNA (+) (red) is much faster than HCV RNA (-) (blue). HCV RNA(-) is known to only function as a replication intermediate, it may never be actively released from the membrane bound replication compartment and therefore be protected from degradation in cytoplasm [28]. The ratio of HCV RNA (+) to HCV RNA (-) in the cytoplasm of hepatocytic cell is approximately 10:1 [16, 57, 58]. Their ratio is approaching 10:1 in this figure which is in accordance with the published studies [16].

3.2. HCV RNA translation

When HCV RNA (+) enters the cell, it is first translated into a single large polyprotein by using IRES, that allows for cap-independent assembly of the 48S ribosomal complex on viral RNA with only a minimal requirement for canonical translation factors [59]. This polyprotein is further subjected to proteosomal cleavage which produces 10 different viral structural and non-structural proteins [42]. The HCV RNA (+) is also used as a template for HCV RNA replication. The switch between replication and translation is not clear for HCV yet but it is speculated in some studies that separate machineries work for replication and translation of the HCV RNA (+) in different compartments of the cell [60]. While others [61] argue that translation and replication occur very close in the cell in a special compartment called replicasome, nevertheless, HCV RNA (+) translation is mediated by both host and viral factors.

In this model the effect of host miR-122 on the translation of NS3/4A protein of the virus was analyzed. The miR-122 is a liver-specific microRNA which is known to stimulate the translation of HCV RNA (+) [62, 63]. The relationship between HCV and miR-122 is quite unusual because normally microRNAs inhibit viral translation and decrease its stability. In the case of HCV, findings suggests that, if miR-122 activity is blocked by sequestering it, HCV RNA (+) translation is reduced significantly [64, 65]. The miR-122 doesn't stimulate the translation of HCV RNA directly, thus this model uses an abstraction of the pathway to include the ultimate effect of the miR-122 on the translation activity of HCV RNA (+). **Figure 3** illustrates miR-122 and its effect on HCV RNA (+) translation. It should be noted that miR-122 is not used up during this process because it only facilitates the translation by increasing the stability of the HCV RNA (+) [28]. **Figure 8** represents the simulation of miR-122 and the relative level of NS3/4A protein. NS3/4A (black) represents the relative level of NS3/4A protein in the cytoplasm of the hepatocytes prior to the positive feedback of the host miR-122 while NS3/4A (red) shows the relative level of NS3/4A protein in the cytoplasm with facilitation by the host miR-122. The miR-122 (blue) is not used up during the process and remains constant. The production rate of viral proteins is thought to be same for all the 10 proteins of HCV because they are produced from a single polyprotein. Thus, only a single protein is shown here for reference. It is clearly evident from **Figure 8** that miR-122 significantly increases the translation activity (NS3/4A protein) of HCV RNA (+). The relative level of the viral protein rises up to a certain level (red and black) with or without miR-122, and then achieves steady state. This is probably due to the

fact that host immune response is activated against the viral RNA (+), which leads to the degradation of the HCV RNA (+). These observations imply that HCV proteins achieve a certain threshold level prior to being blocked at RNA level. The HCV RNA (+) translation is thought to be an inefficient process because HCV tries to persist in the host cell by limiting its other processes such as replication and translation [60]. HCV is also actively involved in self interactions and host-viral interaction in order to limit the antiviral effects of the host [14].
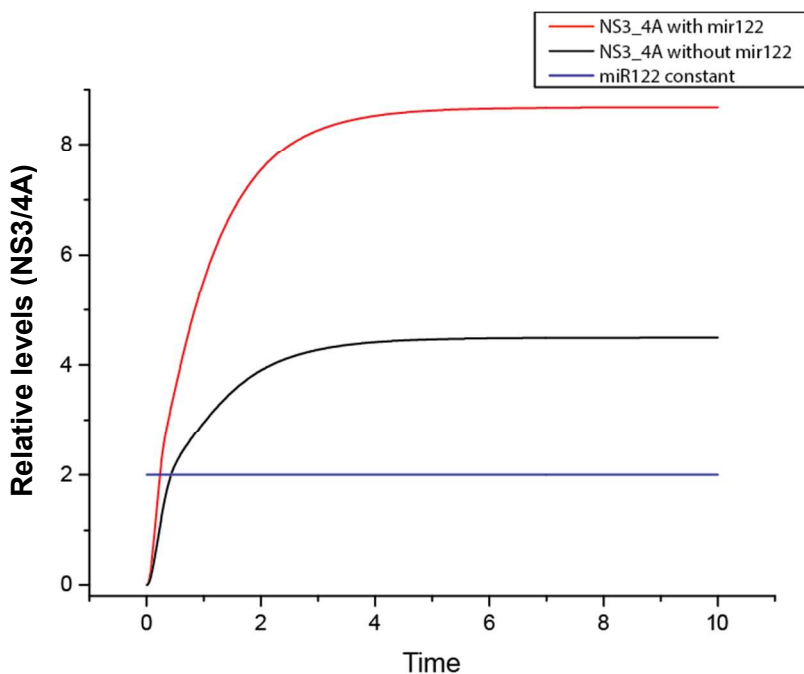

Figure 8: Simulation of HCV RNA (+) translation and effect of host miR-122. X-axis shows the time units while Y-axis shows the relative expression levels. The black line represents the relative level of NS3/4A protein in the cytoplasm of the hepatocytes prior to the positive feedback of the host miR-122; the red line shows the relative level of NS3/4A protein in the cytoplasm with positive effect of the host miR-122; the blue line represents the level of miR-122 in cytoplasm. The miR-122 (blue) is assumed to be present in the host cell and is not used up during the process thus showing a constant horizontal line. The level of production for all viral proteins is thought to be the same because they are produced from a single polyprotein. Thus, only a single protein is shown here for reference. It is clearly evident from **Figure 8** that miR-122 significantly increases the translation activity of HCV RNA (+) almost by 50%. The relative level of the viral protein rises up to a certain level (red and black) with or without miR-122, and then achieves a steady state. A relative increase of approximately 50% observed in the quantity of HCV proteins using simulation of HPN model and shows consensus with published data of laboratory experiments [64].

3.3. HCV RNA inhibition by RNase L

The presence of dsRNA activates innate immune pathways to target and destroy the foreign invasive viruses. RNase L activation is through one of these pathways which degrades RNA (viral and host) at specific residues thus limiting protein synthesis, and ultimately leading to apoptosis[66-68]. RNase L is a latent ribonuclease that is expressed constitutively and ubiquitously in almost all mammalian cells. It activates 2′, 5′-linked oligoadenylate synthetase enzyme (2–5OAS) having an endonuclease activity. Thus, activated RNase L cleaves viral and cellular RNAs at single-stranded regions, resulting in the inhibition of the translation and replication of viral RNA [66]. In addition to the direct antiviral effects of RNase L, an indirect antiviral role for this enzyme has also been suggested. It has been hypothesized that the small RNA fragments that are generated by RNase L can act as a signal for interferon (IFN) production [69].

The impact of RNase L on HCV RNA (+) in the cytoplasm of the hepatocytic cells is studied using HPN. The degradation of HCV RNA (+) is shown as an sink transition activated by RNase L. **Figure 2** illustrates the inhibitory (degradation) effect of RNase L on the HCV RNA (+) in the HPN model. **Figure 9** demonstrates the simulations of HCV RNA (+) with and without the inhibitory effect of RNase L. The black line represents the relative level of HCV RNA (+) in the cytoplasm prior to inhibitory effect of RNase L; the lue line represents the relative level of HCV RNA (+) when RNase L is activated and it degrades the HCV RNA (+); the red line represents the level of RNase L. RNase L (red) being an enzyme is not used up during the process and thus the simulation gives a constant horizontal line. The level of HCV RNA (+) (black) is clearly higher than the level of HCV RNA (+) (blue) subsequent to degradation by RNase L (red). It is observed in the graph that blue line coincides with the black line initially, but afterwards it deviates from its path and rises with a slower rate as compared to the HCV RNA (+) (black). Possible explanation for this phenomenon might be due to the delay in the activation of RNase L enzyme. It also reveals that a certain amount of HCV RNA (+) is required to activate this antiviral enzymatic pathway. The delayed activation allows the HCV RNA (+) (blue) to rise steadily to a certain point, however once the RNase L enzyme is activated and its starts degradation of the viral RNA, the rate of HCV (+) replication is slowed down. The simulations shown in **Figure 9** are in agreement with the observed behavior of RNase L during HCV infection in hepatocytes [69].
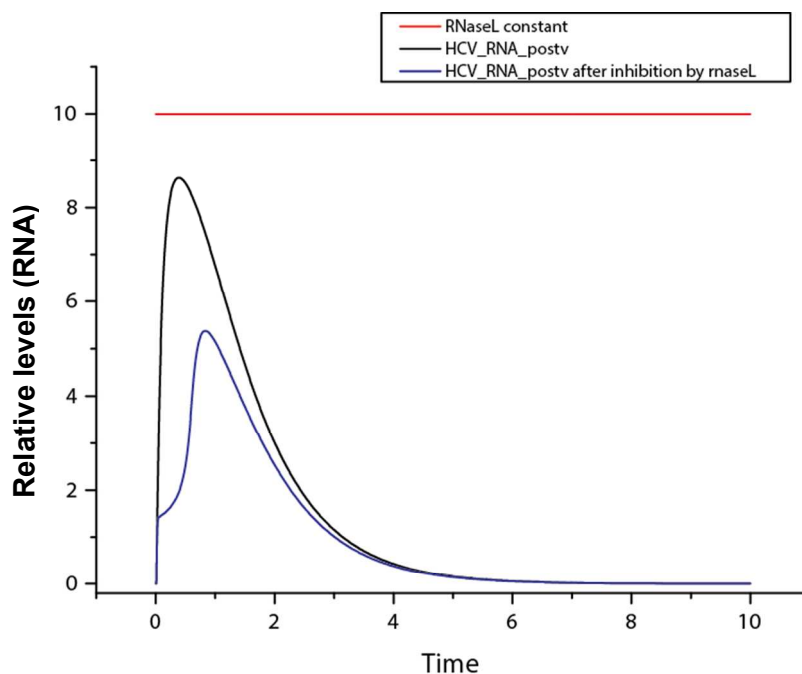
Figure 9: Simulation of HCV RNA (+) with and without the inhibitory effect of RNase L. X-axis represents the time units while Y-axis shows the relative expression levels. The black line represents the relative level of HCV RNA (+) in the cytoplasm preceding inhibitory effect of RNase L; the blue line represents the relative level of HCV RNA (+) when RNase L is activated and it inhibits the HCV RNA (+) by degradation; the red line represents the level of RNase L in the cytoplasm. RNase L (red) being an enzyme is not used up during the process and thus the simulations gives a constant horizontal line. The level of HCV RNA (+) (black) is clearly elevated prior to degradation by RNase L (red), than the level of HCV RNA (+) (blue). It is observed in the above graph that blue line coincides with the black line initially, but later it deviates from its path and rises with a slower rate as compared to the HCV RNA (+) black. It might be due to the delayed activation of the RNase L. The simulation shown in **Figure 9** conform to the observed behavior of RNase L during HCV infection in laboratory experiments [69].

3.4. RIG-1 and TLR3 pathway activation and IFN-β production

TLR3 and RIG-I-like receptors constitute two parallel classes of cellular sensors that recognize viral pathogen associated molecular patterns (PAMP) and initiate innate immune responses [29]. Despite operating via distinct adaptors and mechanisms, both pathways culminate in the activation of IRF3/7-dependent antiviral response and production of NF-κB-dependent pro-inflammatory mediators [29]. Type I IFN plays a central role in eliminating HCV, both under physiological conditions and when used as a therapeutic intervention [56]. Viruses are recognized

by cellular innate immune receptors, such as family of RIG-I–like receptors and TLR3 leading to host antiviral responses, resulting in the production of cytokines such as type I and type III IFNs [56]. RIG-I is activated through recognition of short double-strand RNA (dsRNA) or triphosphate at the 5′ end of dsRNA as pathogen-associated molecular patterns (PAMPs), forming a homo-oligomer that binds with the caspase recruitment domain (CARD) of IPS-1(also known as Cardiff, MAVS or VISA). IPS-1 subsequently recruits TANK binding kinase 1 (TBK1) and IκB kinase ε (IKKε) kinases. Activation of TBK1 and IKKε results in the phosphorylation of IRF-3 or IRF-7, its translocation to the nucleus and the induction of IFN-β mRNA transcription[56, 70, 71]. TLR3 mediates the late phase hepatocellular response to HCV infection by sensing viral dsRNA replicative intermediates, followed by the coupling to adaptor molecule TRIF, which activates cascade of signaling pathway ultimately leading to the production of IFN-β[56]. IFN-β is the first line of defense against viral invasion and it induces several ISGs which contribute to overall antiviral state of the cell. RIG1 pathway is dependent upon interaction with IPS1 while TLR3 pathway is highly dependent upon TRIF adaptor protein for activation and induction of IFN-β and ISGs [29].

The induction of IFN-β and ISGs is illustrated in **Figure 2 and 3** with simulations shown in **Figure 10 and 11.** In **Figure 10**, the red line represents the relative level of IFN-β after activation of RIG-1 and TLR3 pathways. It shows a steady increase in the level of IFN-β in the host cell as a result of TLR3/RIG-1 pathway activation. IFN-β is released outside the cell and in turn it binds to the IFN receptors and leads to the induction of ISGs through JAK/STAT pathway [29]. This phenomenon has an important implication in the chronicity of the HCV infection [29]. The neighboring cells are able to recognize HCV infection by identifying released cytokines and thus limit the infection to the specific area in the liver tissue [29] .

3.5. Inhibition of RIG1 and TLR3 pathways by HCV protein NS3/4A protease

It is a well-established fact that HCV proteins engage rigorously in blocking the antiviral state of the infected cell. For this purpose, RIG-1 and TLR3 pathways are primary targets because they induce the IFN-β production [8]. NS3/4A protease degrades IPS1 adaptor protein, leading to the suppression of the RIG1 mediated IFN-β production [8, 29]. NS3/4A protease also cleaves TRIF adaptor protein in order to inhibit activation of TLR3 pathway, eventually leading to the down

regulation of IFN-β production [8]. It has been reported that the IFN-β promoter activation is reduced by almost 50% in the presence of NS3/4A protease of HCV [25].

We modeled these activities by introducing the inhibitor arcs **(Figure 3)** in the pathway. The simulation results depicted this phenomenon as clearly shown in **Figure 10 and 11**. It was observed that the relative levels of IFN-β and ISGs were significantly reduced after immune pathways are blocked by HCV proteins accumulating in the infected cell. **Figure 10** represents the simulations of the relative levels of IFN-β, before and after inhibition by HCV proteins. The red line represents the relative level of IFN-β before any inhibition occurs by HCV proteins, while the black line represents the IFN-β level following inhibition by HCV NS3/4A protease. The IFN-β (black line) is shown as a flat horizontal line and represents far less production of IFN-β in this model after the TLR3 and RIG-1 pathways are inhibited; however it is not the case during HCV infection in the hepatocytes. Although it is a well-established fact that NS3/4A protease considerably reduces the production of IFN-β [15] but relatively a reduced amount of IFN-β is still detected in the blood stream and surrounding tissues [29]. This model showed little production of IFN-β when TLR3/RIG1 pathways are restricted by NS3/4A protease activity. It is probably due to the inhibition of the flow of tokens very early in the pathway. Coupling it with a weak which does not reach the end products; it is shown as flat (horizontal) line at level (token) zero.
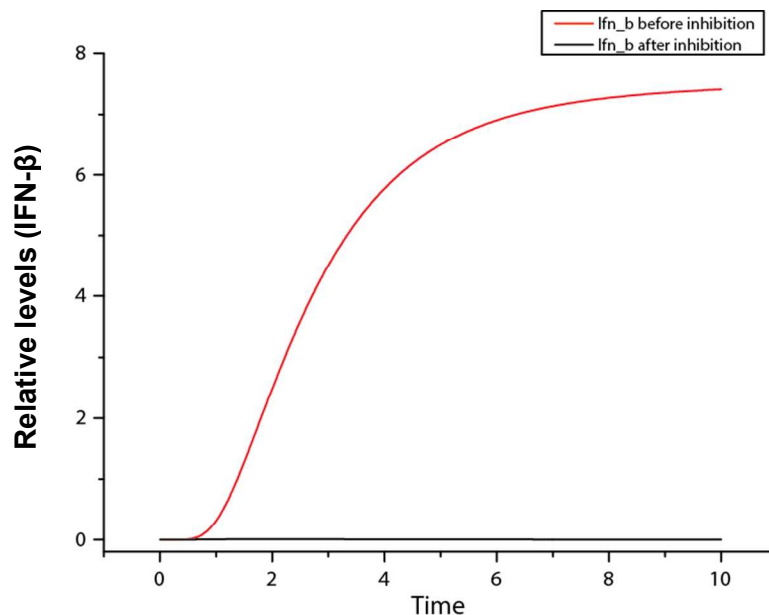
Figure 10: Simulation of IFN-β production before and after inhibition by HCV NS3/4A protease. X-axis represents the time units while Y-axis shows the relative expression levels. The red line represents the relative levels of IFN-β induction by RIG1 and TLR3 pathways when dsRNA intermediates are recognized by the PRRs. The black line represents the relative decrease in IFN-β level after NS3/4A protease degardes TRIF and IPS1 proteins in RIG-1 and TLR3 pathways. The graph shows a clear difference in relative levels of IFN-β with and without the inhibitory effect of HCV NS3/4A protease. Simulation Graph shows no production of IFN-β when TLR3/RIG1 pathways are limited by NS3/4A protease. It is probably due to inhibition of the flow of tokens very early in the pathway, and the signal is so weak that it does not reach the end products.

      Figure 11 represents the simulation result of ISGs, illustrating the relative levels of ISGs before and after inhibition by HCV proteins. The red line represents the relative level of ISGs prior to any inhibitory proteins on the TLR3/RIG-1 pathways. While the black line represents the relative level of ISGs after RIG-1 and TLR3 pathways are inhibited by the NS3/4A protease. The ISGs (black) are in very low concentrations in the cell as compared to ISGs (red), corroborating earlier studies of TLR3 and RIG1 pathway inhibition by HCV proteins [56]. It implicates that HCV has evolved very complex and effective mechanisms to abrogate host antiviral responses and utilizes the host machinery for its own benefit.
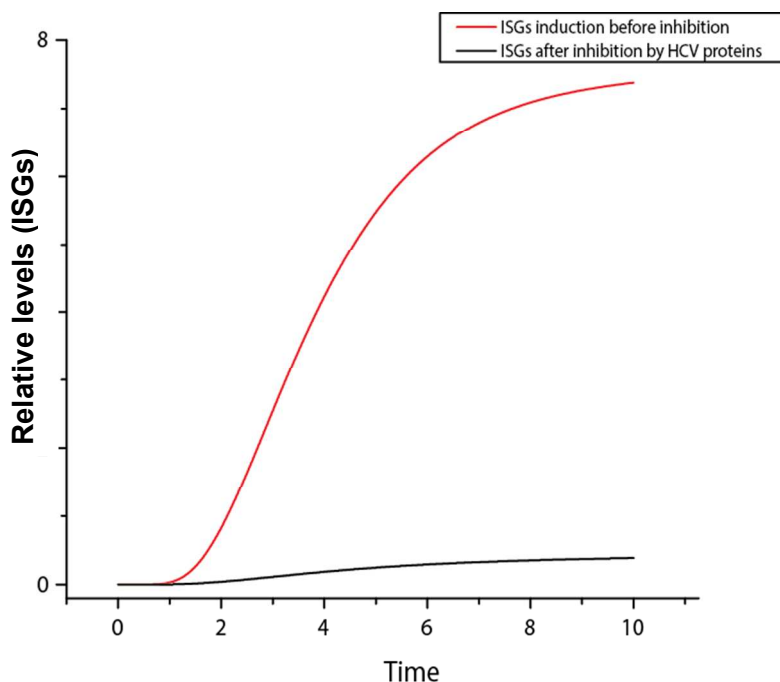
Figure 11: Simulation of ISGs induction before and after inhibition of RIG1 and TLR3 pathways. X-axis represents the time units while Y-axis represents the relative expression levels. The red line represents the relative level of ISGs before any inhibitory proteins acts on the TLR3/RIG-1 pathways; the black line represents the relative level of ISGs after RIG-1 and TLR3 pathways are inhibited by the NS3/4A protease. The ISGs (black) are in very low concentrations in the cell, when TLR3/RIG-1 pathways are inactivated, as compared to ISGs (red) normally produced by cell. These observations corroborate earlier findings involving TLR3 and RIG1 pathway inhibition by HCV proteins [56].

Above results have been summarized in **Table 1**. It clearly shows that non-parametric PN formalism can be applied effectively to study complex human diseases like HCV infection in the hepatocytes. It is a non-parametric study thus, exact concentrations and kinetic knowledge is not required. However, this model can be further extended by the addition of parametric values derived from cell culture experiments or predicted computationally. The resulted simulation data may vary according to the experimental values added for various proteins. Moreover, the behavior of proteins in several other related pathways can be examined in detail by extending this HPN model to related pathways of host innate and adaptive immunity.

Table 1: Summary of the observations reported by experimental methods and their comparison with simulated results.

	Observations	Findings		Citations
		Experimental	Model simulation	
01	HCV RNA ratio in the cell	10:1	~10:1	16, 57, 58
02	microRNA-122 effect on HCV RNA translation	+	+	64
03	Effect of NS3/4A protease on IFN-β production	–	– –	61
04	Effect of RNase L on HCV RNA level	–	–	69
05	Effect on IFN-β production as a result of HCV infection	+	+	43, 71
06	Effect on Interferon stimulated genes (ISGs) induction as a result of HCV infection	+	+	29
07	Effect of NS3/4A protease on ISGs expression	–	–	72
08	Effect of NS3/4A protease on TLR3-TRIF complex	–	–	73
09	Regulation of RNase L by HCV proteins (NS5A)	–	–	69
10	Effect of NS3/4A protease on RIGI-IPS1/MAVS signalosome	–	–	23, 25, 29
11	Effect of HCV proteins on NF-kβ induction	–	–	74

Symbols represent changes in expression levels of observed proteins within HCV infection pathway. + represents the upregulation while – represents down-regulation of the entities/proteins. -- increased inhibition.

3.6. Simulating Protein Kinase R Perturbration:

A perturbration experiment was designed to extend our model and study the role of Protein kinase R (PKR) in HCV infection pathway **(Supplementary file 3)** . Perturbrations can include knockout of genes, inhibition of proteins or changes in external stimuli. These perturbrations can be studied in the PN by addition or removal of various arcs and source/sink transitions. Nevertheless, it depends upon the user and the experiment being performed.

PKR is considered as one of the major player and critical mediator in the antiviral action of IFN, as an IFN-induced, dsRNA-activated protein kinase can control protein synthesis, [75, 76],[77]. PKR participates in several cellular signaling pathways in response to stress signals via controlling protein translation through eIF2α (a cellular substrate of PKR) phosphorylation,

mainly as a result of viral infections [76]. Not only is the PKR an effector molecule of the cellular response to double-stranded RNA, it is also implicated in other regulatory pathways, including those activating p53, p38, IRF-1 and NF-κB [78].

PKR has been recently implicated as pro-HCV kinase [27] because the eIF2α activation is beneficial for HCV as it limits the ISGs' mRNA translation resulting in increased proliferation of viral RNA and virion particles. It is in accordance with the observation that many patients have increased level of ISGs mRNA but the HCV propagation and replication is not limited. This hypothesis of pro-HCV PKR is also supported in another study by Weiland S *et al.* [31]. In addition, it is also reported that E2 and NS5A proteins of HCV interact with PKR and inhibits its activity [79, 80]. These observations implicate that there is a critical balance between the dual roles of PKR in HCV infection. Due to its intrinsic properties, PKR has been studied extensively to document its relevance as a cell's first line of defense mechanism against viral infections and as a growth regulator [81].

We extended our model by introducing PKR pathway and interconnecting it with HCV replication cycle, translational control in cell and inhibiting antiviral property of ISGs and IFN-β (**Supplementary File 3**). Its behaviour was studied in both the cases when HCV is being "normally" inhibited (**Figure 2**) as compared to the pathway when HCV takes control of cellular machinery (**Figure 3**). Analysis of the resulting simulations (**Supplementary File 3, 4, 5**) reveal that the role of PKR is more salient during the early acute infection of HCV. i.e. HCV has not fully established itself in the host cell. Observing several mechanisms and effector functions of PKR implicates that if ISGs are already activated (high basal level) in the cell, it results in the activation of PKR thus activating the translational control. So, when HCV infects, IFN-β and ISGs cannot be translated. Consequently, viral replication and virion production cannot be limited within the host cell. HCV has cap-independent translation thus it eventually evades the translation control within host cell. In the case of established HCV infection, viral protease effeciently blocks RIG1 and TLR3 pathways, thus the pro-viral effect of PKR is not profound. Upon literature survey, it was found to be reported that ISG15 activates PKR in the absence of any infection[82]. It is a gain of function mutation which results in auto-phosphorylation and subsequent activation of PKR. Although it is one of the mechanism for activation of PKR, it supports the findings of our model (**Supplementary File 3, 4, 5**) that an alternate pathway may exist for PKR activation which leads to proliferation of HCV despite activation and transcription

of immune response elements. It might help to explain why many patients fail to clear acute HCV infection while others with low ISGs basal levels clear HCV spontaneously.

This case for the pathological consequences of the antiproliferative or pro-proliferative action of PKR is less understood and out of scope for our current study. Nevertheless, it is intriguing phenomenon and targeting PKR might be a rational therapeutic strategy which can offer promising results.

4. Conclusion

Our proposed methodology efficiently predicted the changes in enzyme activities and protein levels in response to various alterations in the stimuli inside the hepatocytes. It is imperative for biologists to derive information about a network's dynamic behavior without extensive experimentation and exhaustive computational parameter estimation. PN formalism offers scientists the exciting prospect of being able to test hypotheses regarding signal propagation *in silico*. In western blot and microarray experiments, biologist prefer the use of "up" and "down" regulation to report observations during cell culture experiments because it is less likely to be influenced by extraneous variables. Keeping these interpretations in mind, we have successfully developed a HPN model encompassing the important HCV infection steps and innate immune response elements and perturbation experiment analyzing the role of PKR in HCV infection pathway. The resultant simulations are in agreement with the published experimental findings. Although, the accurate prediction of the concentrations relies on quantitative data, our model showed good results for predicting responses by introduction or removal of inhibitory pathways. This model can be further extended to encompass adaptive immune response to HCV infection and to study pathological consequences of various proteins as well. The strategy used here is straightforward, user friendly and can be easily applied to other similar cases.

Acknowledgements

References

1. Q. L. Choo, G. Kuo, A. J. Weiner, L. R. Overby, D. W. Bradley and M. Houghton, *Science*, 1989, 244, 359.
2. J. Bukh, R. H. Miller and R. H. Purcell, *Semin Liver Dis*, 1995, 15, 41-63.
3. D. B. Smith, J. Bukh, C. Kuiken, A. S. Muerhoff, C. M. Rice, J. T. Stapleton and P. Simmonds, *Hepatology*, 2014, 59, 318-327.
4. M. G. Ghany and N. Gara, *The Lancet*, 2014.
5. K. Mohd Hanafiah, J. Groeger, A. D. Flaxman and S. T. Wiersma, *Hepatology*, 2013, 57, 1333-1342.
6. G. M. Lauer, *Journal of Infectious Diseases*, 2013, 207, S7-S12.
7. J. G. McHutchison, E. J. Lawitz, M. L. Shiffman, A. J. Muir, G. W. Galler, J. McCone, L. M. Nyberg, W. M. Lee, R. H. Ghalib and E. R. Schiff, *New England Journal of Medicine*, 2009, 361, 580-593.
8. S. M. Horner and M. Gale Jr, *Nature medicine*, 2013, 19, 879-888.
9. M. H. Heim, *Nature Reviews Immunology*, 2013, 13, 535-542.
10. B. Al-Bawardy, W. Kim, J. J. Poterucha, J. B. Gross, M. R. Charlton, J. J. Larson, C. L. Colby, K. Canterbury, J. Warner and T. M. Therneau, 2014.
11. B. Gao, F. Hong and S. Radaeva, *Hepatology*, 2004, 39, 880-890.
12. M. Lechmann, K. Murata, J. Satoi, J. Vergalla, T. F. Baumert and T. J. Liang, *Hepatology*, 2001, 34, 417-423.
13. R. Thimme, M. Binder and R. Bartenschlager, *FEMS microbiology reviews*, 2012, 36, 663-683.
14. P. Georgel, C. Schuster, M. B. Zeisel, F. Stoll-Keller, T. Berg, S. Bahram and T. F. Baumert, *Trends in molecular medicine*, 2010, 16, 277-286.
15. L. Chatel-Chaix, M. Baril and D. Lamarre, *Viruses*, 2010, 2, 1752-1765.
16. H. Dahari, R. M. Ribeiro, C. M. Rice and A. S. Perelson, *Journal of virology*, 2007, 81, 750-760.
17. B. H. Junker and F. Schreiber, *Analysis of biological networks*, John Wiley & Sons, 2011.
18. N. L. Novere, A. Finney, M. Hucka, U. S. Bhalla, F. Campagne, J. Collado-Vides, E. J. Crampin, M. Halstead, E. Klipp and P. Mendes, *Nature Biotechnology*, 2005, 23, 1509-1515.
19. R. Thomas and R. d'Ari, *Biological feedback*, CRC press, 1990.
20. R. David and H. Alla, *Discrete, continuous, and hybrid Petri nets*, Springer Science & Business Media, 2010.
21. A. Richard, G. Rossignol, J.-P. Comet, G. Bernot, J. Guespin-Michel and A. Merieau, *PLoS One*, 2012, 7, e24651.
22. A. Sackmann, M. Heiner and I. Koch, *BMC bioinformatics*, 2006, 7, 482.
23. M. Baril, M.-E. Racine, F. Penin and D. Lamarre, *Journal of virology*, 2009, 83, 1299-1311.
24. M. Binder, N. Sulaimanov, D. Clausznitzer, M. Schulze, C. M. Hüber, S. M. Lenz, J. P. Schlöder, M. Trippler, R. Bartenschlager and V. Lohmann, *PLoS pathogens*, 2013, 9, e1003561.
25. A. Breiman, N. Grandvaux, R. Lin, C. Ottone, S. Akira, M. Yoneyama, T. Fujita, J. Hiscott and E. F. Meurs, *Journal of virology*, 2005, 79, 3969-3978.
26. L. Buonaguro, A. Petrizzo, M. L. Tornesello and F. M. Buonaguro, *Infectious agents and cancer*, 2012, 7, 1-12.
27. U. Garaigorta and F. V. Chisari, *Cell host & microbe*, 2009, 6, 513-522.
28. A. García-Sastre and M. J. Evans, *Proceedings of the National Academy of Sciences*, 2013, 110, 1571-1572.
29. M. H. Heim, *Journal of hepatology*, 2013, 58, 564-574.
30. Y.-C. Kwon, J.-I. Kang, S. B. Hwang and B.-Y. Ahn, *FEBS letters*, 2013, 587, 156-164.

31. S. Wieland, Z. Makowska, B. Campana, D. Calabrese, M. T. Dill, J. Chung, F. V. Chisari and M. H. Heim, *Hepatology*, 2014, 59, 2121-2130.
32. C. Chaouiya, *Briefings in bioinformatics*, 2007, 8, 210-219.
33. M. Heiner, M. Herajy, F. Liu, C. Rohr and M. Schwarick, in *Application and Theory of Petri Nets*, Springer, 2012, pp. 398-407.
34. S. Hardy and P. N. Robillard, *Journal of bioinformatics and computational biology*, 2004, 2, 619-637.
35. M. Blätke, M. Heiner and W. Marwan, *Tutorial Petri Nets in Systems Biology*, Technical Report, Otto-von-Guericke University, Magdeburg, 2011.
36. J. W. Pinney, D. R. Westhead and G. A. McConkey, *Biochemical Society Transactions*, 2003, 31, 1513-1515.
37. C. Li, S. Suzuki, Q.-W. Ge, M. Nakata, H. Matsuno and S. Miyano, *Journal of bioinformatics and computational biology*, 2006, 4, 1119-1140.
38. D. Ruths, M. Muller, J.-T. Tseng, L. Nakhleh and P. T. Ram, *PLoS computational biology*, 2008, 4, e1000005.
39. M. Heiner and I. Koch, in *Applications and Theory of Petri Nets 2004*, Springer, 2004, pp. 216-237.
40. M. Kanehisa, S. Goto, Y. Sato, M. Kawashima, M. Furumichi and M. Tanabe, *Nucleic acids research*, 2014, 42, D199-D205.
41. R. Z. Paracha, J. Ahmad, A. Ali, R. Hussain, U. Niazi, S. H. K. Tareen and B. Aslam, *PLoS One*, 2014, 9, e108466.
42. J. Dubuisson, F. Helle and L. Cocquerel, *Cellular microbiology*, 2008, 10, 821-827.
43. T. Saito and M. Gale, *Hepatology Research*, 2008, 38, 115-122.
44. T. Taguchi, M. Nagano-Fujii, M. Akutsu, H. Kadoya, S. Ohgimoto, S. Ishido and H. Hotta, *Journal of general virology*, 2004, 85, 959-969.
45. P. Pileri, Y. Uematsu, S. Campagnoli, G. Galli, F. Falugi, R. Petracca, A. J. Weiner, M. Houghton, D. Rosa and G. Grandi, *Science*, 1998, 282, 938-941.
46. M. B. Zeisel, G. Koutsoudakis, E. K. Schnober, A. Haberstroh, H. E. Blum, F. L. Cosset, T. Wakita, D. Jaeck, M. Doffoel and C. Royer, *Hepatology*, 2007, 46, 1722-1731.
47. M. J. Evans, T. von Hahn, D. M. Tscherne, A. J. Syder, M. Panis, B. Wölk, T. Hatziioannou, J. A. McKeating, P. D. Bieniasz and C. M. Rice, *Nature*, 2007, 446, 801-805.
48. S. Liu, W. Yang, L. Shen, J. R. Turner, C. B. Coyne and T. Wang, *Journal of virology*, 2009, 83, 2011-2014.
49. N. Pavio and M. M. Lai, *Journal of biosciences*, 2003, 28, 287-304.
50. G. A. Otto and J. D. Puglisi, *Cell*, 2004, 119, 369-380.
51. A. P. Roberts, A. P. Lewis and C. L. Jopling, *Nucleic acids research*, 2011, 39, 7716-7729.
52. S. A. Shiryaev, E. R. Thomsen, P. Cieplak, E. Chudin, A. V. Cheltsov, M. S. Chee, I. A. Kozlov and A. Y. Strongin, *PLoS One*, 2012, 7, e35759.
53. J. Ahmad, U. Niazi, S. Mansoor, U. Siddique and J. Bibby, *PLoS One*, 2012, 7, e33532.
54. J. Ahmad, O. Roux, G. Bernot and J.-P. Comet, *International journal of bioinformatics research and applications*, 2008, 4, 240-262.
55. E. M. Clarke, O. Grumberg and D. Peled, *Model checking*, MIT press, 1999.
56. H. M. Liu and M. Gale, *Gastroenterology research and practice*, 2011, 2010.
57. M. Chang, O. Williams, J. Mittler, A. Quintanilla, R. L. Carithers Jr, J. Perkins, L. Corey and D. R. Gretch, *The American journal of pathology*, 2003, 163, 433-444.
58. D. Quinkert, R. Bartenschlager and V. Lohmann, *Journal of virology*, 2005, 79, 13594-13605.
59. P. J. Lukavsky, *Virus research*, 2009, 139, 166-171.
60. S.-L. Tan, *Hepatitis C Viruses: Genomes and molecular biology*, Horizon Scientific Press, 2006.

61.   H. M. Liu, H. Aizaki, K. Machida, J.-H. J. Ou and M. M. Lai, *PLoS One*, 2012, 7, e43600.
62.   J. I. Henke, D. Goergen, J. Zheng, Y. Song, C. G. Schüttler, C. Fehr, C. Jünemann and M. Niepmann, *The EMBO journal*, 2008, 27, 3300-3310.
63.   C. L. Jopling, M. Yi, A. M. Lancaster, S. M. Lemon and P. Sarnow, *Science*, 2005, 309, 1577-1581.
64.   R. K. Jangra, M. Yi and S. M. Lemon, *Journal of virology*, 2010, 84, 6615-6625.
65.   H. L. Janssen, H. W. Reesink, E. J. Lawitz, S. Zeuzem, M. Rodriguez-Torres, K. Patel, A. J. van der Meer, A. K. Patick, A. Chen and Y. Zhou, *New England Journal of Medicine*, 2013, 368, 1685-1694.
66.   R. H. Silverman, *Journal of virology*, 2007, 81, 12720-12729.
67.   L. Zhao, B. K. Jha, A. Wu, R. Elliott, J. Ziebuhr, A. E. Gorbalenya, R. H. Silverman and S. R. Weiss, *Cell host & microbe*, 2012, 11, 607-616.
68.   R. H. Silverman, *Cytokine & growth factor reviews*, 2007, 18, 381-388.
69.   K. Malathi, B. Dong, M. Gale and R. H. Silverman, *Nature*, 2007, 448, 816-819.
70.   T. Saito, R. Hirai, Y.-M. Loo, D. Owen, C. L. Johnson, S. C. Sinha, S. Akira, T. Fujita and M. Gale, *Proceedings of the National Academy of Sciences*, 2007, 104, 582-587.
71.   M. Yoneyama, M. Kikuchi, T. Natsukawa, N. Shinobu, T. Imaizumi, M. Miyagishi, K. Taira, S. Akira and T. Fujita, *Nature immunology*, 2004, 5, 730-737.
72.   Y.-M. Loo, D. M. Owen, K. Li, A. K. Erickson, C. L. Johnson, P. M. Fish, D. S. Carney, T. Wang, H. Ishida and M. Yoneyama, *Proceedings of the National Academy of Sciences*, 2006, 103, 6001-6006.
73.   K. Li, E. Foy, J. C. Ferreon, M. Nakamura, A. Ferreon, M. Ikeda, S. C. Ray, M. Gale and S. M. Lemon, *Proceedings of the National Academy of Sciences of the United States of America*, 2005, 102, 2992.
74.   K. Li and S. M. Lemon, 2013.
75.   L. Zhang, H. J. Alter, H. Wang, S. Jia, E. Wang, F. M. Marincola, J. W. Shih and R. Y. Wang, *Virology*, 2013, 438, 28-36.
76.   R. Toroney, S. R. Nallagatla, J. A. Boyer, C. E. Cameron and P. C. Bevilacqua, *J Mol Biol*, 2010, 400, 393-412.
77.   S. Dabo and E. F. Meurs, *Viruses*, 2012, 4, 2598-2635.
78.   J.-I. Kang, S.-N. Kwon, S.-H. Park, Y. K. Kim, S.-Y. Choi, J. P. Kim and B.-Y. Ahn, *Virus research*, 2009, 142, 51-56.
79.   M. Gale, C. M. Blakely, B. Kwieciszewski, S.-L. Tan, M. Dossett, N. M. Tang, M. J. Korth, S. J. Polyak, D. R. Gretch and M. G. Katze, *Molecular and cellular biology*, 1998, 18, 5208-5218.
80.   D. R. Taylor, S. T. Shi, P. R. Romano, G. N. Barber and M. M. Lai, *Science*, 1999, 285, 107-110.
81.   M. A. Garcia, J. Gil, I. Ventoso, S. Guerra, E. Domingo, C. Rivas and M. Esteban, *Microbiol Mol Biol Rev*, 2006, 70, 1032-1060.
82.   F. Okumura, A. J. Okumura, K. Uematsu, S. Hatakeyama, D.-E. Zhang and T. Kamura, *Journal of Biological Chemistry*, 2013, 288, 2839-2847.
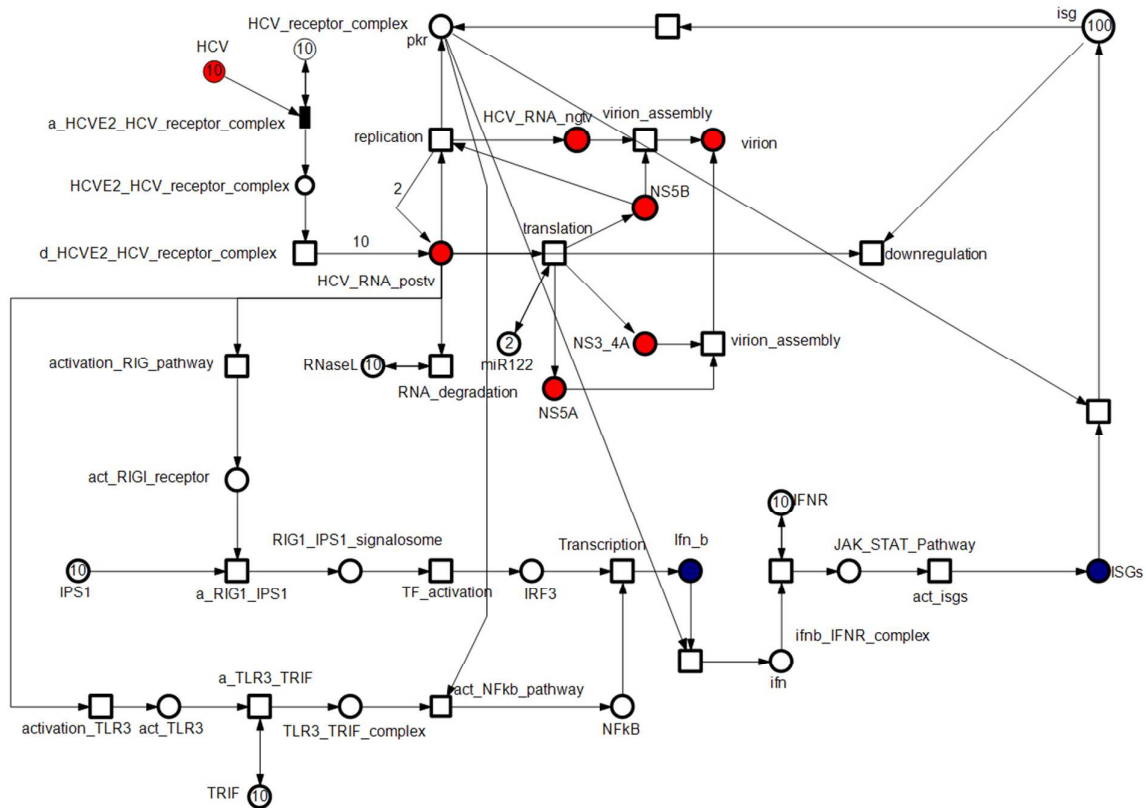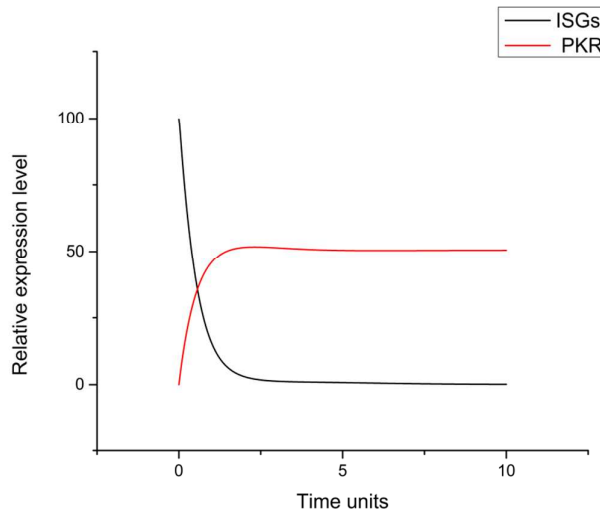
Supplementary file 1:
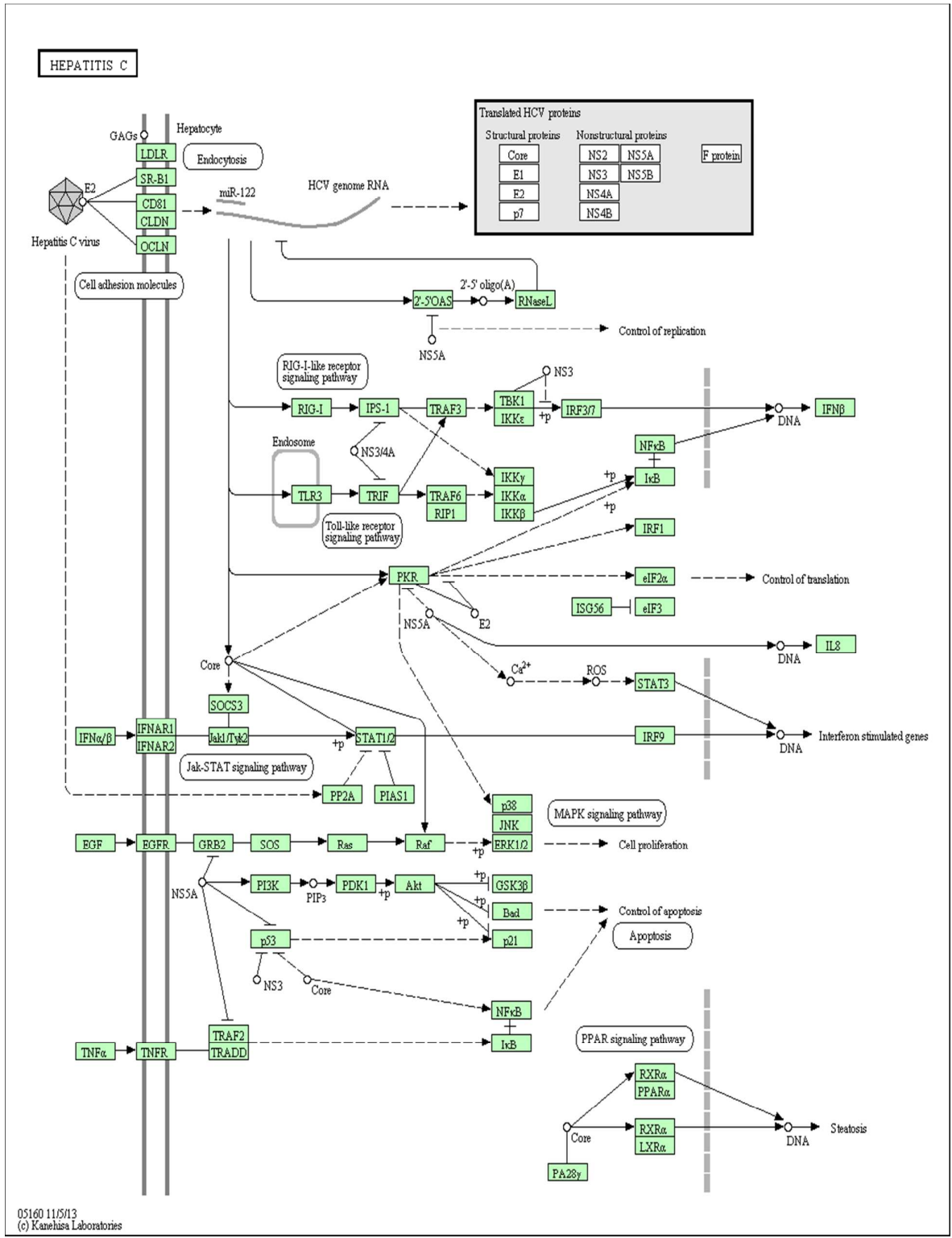
Supplementary File 2:
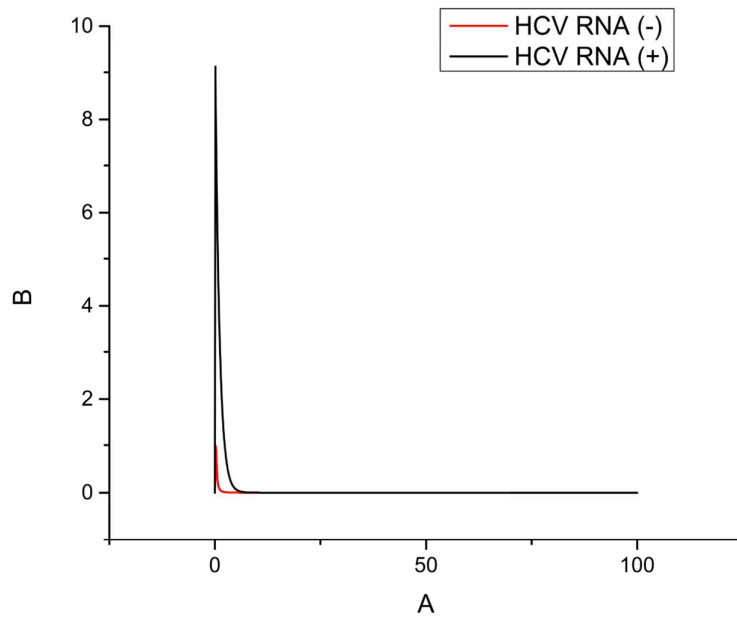
Supplementary File 2: **Simulation result for 100 time units**: Relative concentration of HCV RNA (+) and HCV RNA (-) represented on y-axis with time units on x-axis. The entities achieve a steady state after initial oscillations. As observed, the behavior does not change and remains stable for 100 time units.
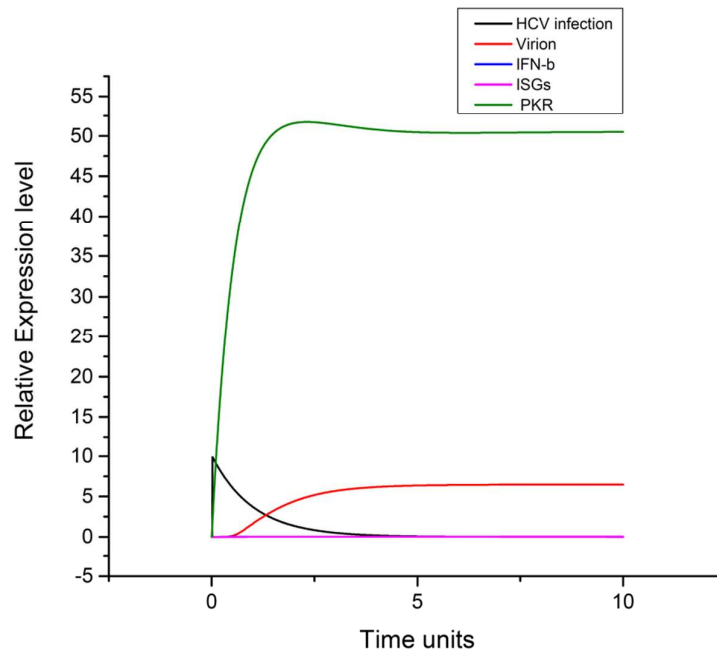
Supplementary File 3:

Supplementary File 3: Illustration of the HPN model elucidating the role of Protein Kinase R (PKR) in HCV infection pathway. Token concentration of ISGs was increased in order to show their high basal level resulting in PKR activation prior to HCV infection in the hepatocytes. PKR activation results in the overall translational suppression in the cell, assisting HCV proliferation. A standard place is illustrated as a circle ○ representing HCV proteins, cellular enzymes, and receptor complexes. Red places represent important HCV proteins selected for this study , while blue places represent important end products of host immune responses selected for this study in particular.. A continuous transition is depicted as ☐ representing all cellular processes including endocytosis, exocytosis, transcription, translation and activation. A ⟶ directed arc connects a place with a transition and vice versa.
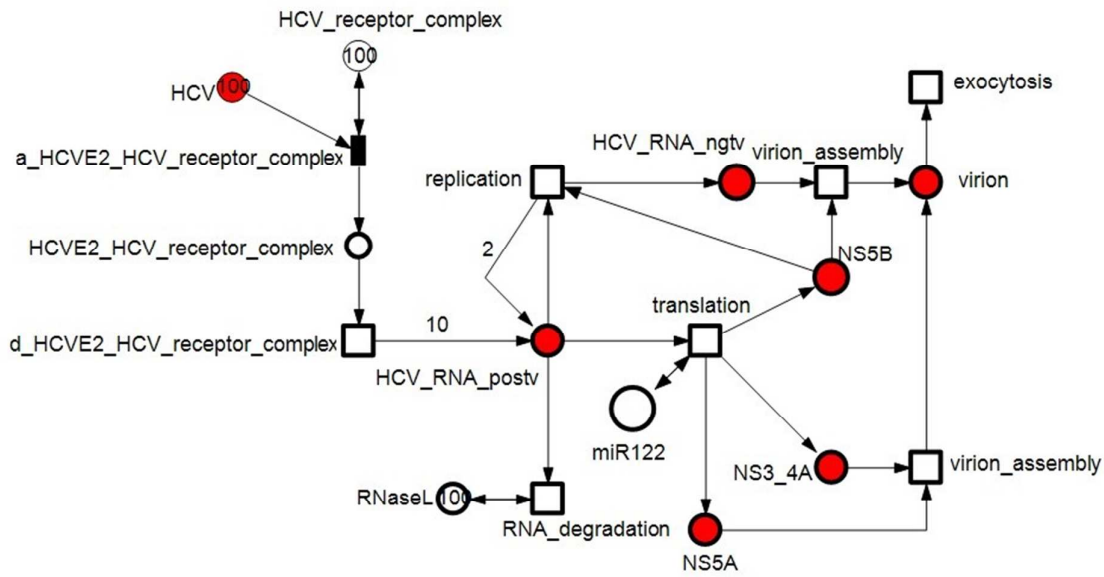
Supplementary File 4:

Supplementary File 4: Relative expression and activation of PKR in the cell prior to HCV infection: X-axis shows time units, while y-axis represents relative expression levels of ISGs and PKR. In certain non-responder patients, ISGs are already activated due to some other infection in body, which might result in activation of PKR [82]. Black line represents ISGs while red line represents activation of PKR. As the signal is transferred from ISGs to PKR thus black line shows a gradual decrease while red line shows a relative gradual increase in concentration, representing activation of PKR to maintain a basal activation level of PKR prior to acute HCV infection.
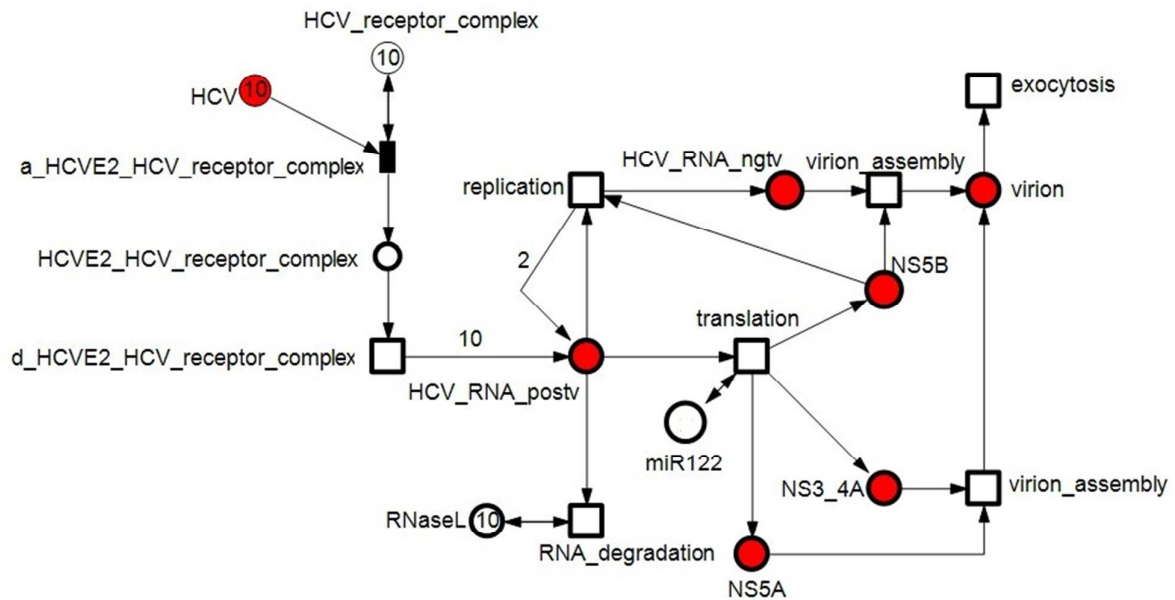
Supplementary file 5:

Supplementary file 5: **Relative expression levels of PKR, IFN-β, ISGs and virion during acute HCV infection**: X-axis shows time units while y-axis represents relative expression levels. The black line represents HCV infectious particles, the red line represents virion production, the green line represents PKR activation, the pink line and the blue line represents ISGs and IFN-β respectively. As soon as acute infection of HCV occurs, IFN-β and ISGs induction does not occur in substantial amount (pink line) to induce effective immune response. As shown in the graph, virion level (red) increases steadily while IFN-β and ISGs (pink) are not expressed due to translational control exhibited by PKR (green).
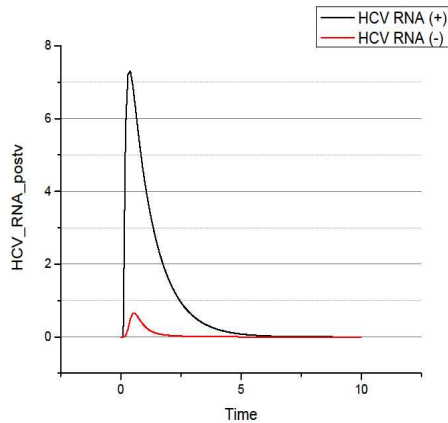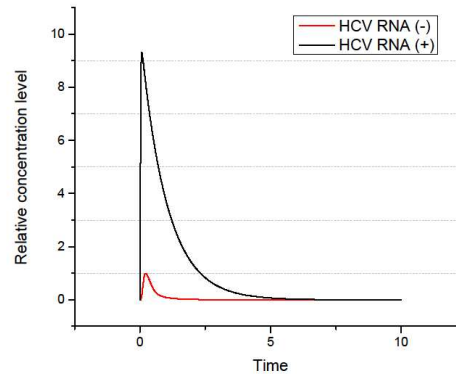
Supplementary file 6 A:

6B:

Supplementary File 6 A & B: Illustration of HCV entry and replication with 10 and 100 tokens. Figure 6A & 6B represent illustration of the simplified PN model showing HCV entry and replication of its genome. In order to clarify our point, we have shown below (Figure 6C & 6D), simulation graphs for both 6A and 6B, with 10 tokens and 100 tokens respectively. A standard place is illustrated as a circle ○ representing HCV proteins, cellular enzymes, and receptor complexes. Red places represent important HCV proteins selected for this study , while blue places represent important end products of host immune responses selected for this study in particular.. A continuous transition is depicted as □ representing all cellular processes including endocytosis,

exocytosis, transcription, translation and activation. A ——————➤ directed arc connects a place with a transition and vice versa.

6C :   **6D:**

Supplementary file 6 C & 6D: **Simulation graphs for relative concentration of HCV RNA (+) and HCV RNA (-) in the cell** having 10 and 100 tokens. X-axis represents time units while y-axis shows relative concentration level. Figure 6C and 6D shows that varying the tokens does not change the relative ratio (~10:1) of the entities.

Supplementary File 7, Source files (zip-archive)